

# ENDOGENOUS POVERTY TRAPS IN CONTINUOUS TIME: A SIGNALING APPROACH

MASSIMO GIANNINI<sup>1</sup>

Department of Enterprise Engineering, University of Rome Tor Vergata

This paper embeds a signaling friction into the continuous-time heterogeneous agent framework. A continuum of producers operate Cobb-Douglas technologies with regime-specific productivity  $A_j \in \{A_L, A_H\}$ . Stochastic arrival of signaling opportunities and skill obsolescence risk generate an optimal stopping problem—when to pay a lump-sum cost  $\phi$  to upgrade productivity—whose solution yields an endogenous Skiba threshold  $k^*$ . Diminishing returns create a stable interior attractor in each regime; the signaling cost separates the two basins, producing a poverty trap that is an interior optimum rather than a corner solution. The stationary distribution exhibits Twin Peaks, but its decomposition by regime reveals that agents in three distinct states—structurally trapped, waiting to signal, and successfully upgraded—coexist at the same wealth levels with different consumption behavior and mobility prospects. Capital alone is therefore insufficient to identify an agent’s position in the polarization dynamics. We show that the joint observation of a low marginal propensity to consume out of wealth and a high average propensity to consume—a combination invisible to standard Euler equation tests—is the diagnostic signature of the structural trap, distinguishing it from both liquidity constraints and transitory shocks.

KEYWORDS: Poverty traps, heterogeneous agents, signaling frictions, Twin Peaks, optimal stopping, marginal propensity to consume, metastability, viscosity solutions.

JEL CLASSIFICATION: C61, D31, D82, E21, O15.

## 1. INTRODUCTION

The persistence of wealth polarization remains one of the most resilient puzzles in macroeconomics. Despite the convergence predictions of the neoclassical growth model, empirical wealth distributions exhibit a stubborn bimodality—often characterized as “Twin Peaks”—where a significant portion of the population clusters near a low-wealth attractor while another converges to a high-wealth club (Quah, 1996, 1997).

Standard Heterogeneous Agent models, following Aiyagari (1994) and Bewley (1986), generate wealth dispersion through idiosyncratic income shocks and precautionary savings. In these frameworks, inequality is essentially a phenomenon of luck: given enough time and positive transition probabilities, the economy is ergodic and social mobility is inevitable. This narrative struggles to explain the structural entrenchment of poverty observed in dual economies, where barriers to mobility appear not merely stochastic but systemic.

This paper provides a structural theory of endogenous inequality by embedding a signaling friction into the continuous-time Heterogeneous Agent framework of Achdou et al. (2022). A continuum of producers each operate a Cobb-Douglas technology  $y_i = A_j k_i^\alpha$  with diminishing returns ( $\alpha < 1$ ) and regime-specific productivity  $A_j \in \{A_L, A_H\}$ . The low state  $A_L$  represents the baseline technology available to those who lack a recognized credential or occupy routine occupations; the high state  $A_H$  represents the frontier technology accessible to those who have successfully invested in a skill upgrade.

---

Massimo Giannini<sup>1</sup>: [massimo.giannini@uniroma2.it](mailto:massimo.giannini@uniroma2.it)

<sup>1</sup>This work builds upon a strand of research initiated in the early 2000s when I was a visiting PhD student at Nuffield College, University of Oxford. I was encouraged and supported to pursue research in the field of inequality by my supervisor and mentor, Sir Anthony Atkinson. Although he is no longer with us, this work is the fruit of our extensive discussions and his teachings. Thank you, Tony, wherever you are.

Transitions between regimes are stochastic and capture the Schumpeterian idea that economic progress is driven by long waves of creation and destruction. Signaling opportunities arrive at Poisson rate  $\lambda_{LH}$ —the emergence of a new paradigm, the opening of a training program, or a regulatory reform that creates demand for a new credential—making it feasible for an L-agent to upgrade to  $A_H$ . Skill obsolescence strikes at rate  $\lambda_{HL}$ —technological displacement, the commoditization of a once-scarce skill—reverting productivity from  $A_H$  to  $A_L$ . Crucially, the decision to exercise a signaling opportunity is endogenous: the agent chooses when to pay a lump-sum cost  $\phi$  from her capital stock, generating an optimal stopping problem of American option type.

The signaling structure builds on [Giannini \(2003\)](#), where workers’ human capital is private information and the informational asymmetry produces a pooled wage for uncredentialed workers and individual matching for credentialed ones. Our framework inherits this logic in reduced form:  $A_L$  corresponds to the pooling equilibrium,  $A_H$  to the separating equilibrium, and  $\phi$  to the educational investment required to reveal one’s type. This interpretation is consistent with, but does not require, the specific bargaining structure of [Giannini \(2003\)](#); alternative micro-foundations would generate the same reduced-form structure.

The interaction between the signaling friction, the stochastic environment, and diminishing returns partitions the population into three behavioral regimes. An agent in *state L* has no signaling opportunity and faces a standard consumption-savings problem with a unique attractor  $k_L^{ss,c}$  where the risk-adjusted marginal return to saving equals the discount rate. An agent in *state W* has received an opportunity but not yet exercised it. She produces at  $A_L$  but holds the option to pay  $\phi$  and jump to  $A_H$ . The tension between signaling quickly (before the opportunity expires at rate  $\lambda_{HL}$ ) and accumulating enough capital for the transition to be worthwhile generates an endogenous Skiba threshold  $k^*$ : below it, the agent waits; above it, she signals immediately. Agents in the interval  $[\phi, k^*)$ —able to afford  $\phi$  but rationally choosing to wait—are the “Frustrated Aspirants” of our taxonomy. An agent in *state H* has paid  $\phi$  and produces at  $A_H$ , but faces ongoing obsolescence risk. This risk generates two opposing forces: a front-loading effect (consume more while income is high) and a precautionary saving effect (accumulate a buffer against income loss). Under our calibration the precautionary motive dominates, so  $k_H^{ss,c}$  lies above the deterministic benchmark. When the obsolescence shock hits, the agent reverts to  $A_L$  at high wealth and becomes a “Decaying Rentier,” over-consuming relative to her low-productivity income as she slides back toward  $k_L^{ss,c}$ .

The paper makes three contributions to the literature on poverty traps.

*First*, the model produces a structurally distinct form of poverty trap—one where agents are at an interior optimum, not at a binding constraint. At  $k_L^{ss,c}$ , diminishing returns have driven the risk-adjusted marginal return to saving down to the discount rate. The agent is not constrained; she is rationally immobile. The trap arises from the optimality of the agent’s own behavior, not from an external barrier.

*Second*, we identify a consumption signature that is invisible to standard tests: low MPC out of wealth ( $\partial c/\partial k \approx \rho$ ) combined with high APC ( $c/Y \approx 0.90$ ). At the zero-drift attractor, the agent has no incentive to save a windfall—the net marginal return is approximately  $\rho$ —so the transfer is absorbed into consumption while capital remains at  $k_L^{ss,c}$ . An econometrician using the MPC alone would classify her as unconstrained; using the APC alone would suggest financial stress. Only the joint observation reveals the trap. In the taxonomy of [Kaplan and Violante \(2014\)](#), these agents resemble the wealthy hand-to-mouth in one dimension (high APC, negligible net saving) but differ sharply in another: their MPC is low, not high. They are not hitting a wall (a binding constraint); they are sitting in a hole (a low-productivity basin from which the returns to saving cannot lift them out). The wall is visible to standard tests. The hole is not.

*Third*, the decomposition of the stationary distribution by regime reveals that agents in three distinct states—structurally trapped, waiting to signal, and successfully upgraded—coexist at the same wealth levels with radically different consumption behavior and mobility prospects. Capital alone is therefore insufficient to identify an agent’s position in the polarization dynamics: two households with identical wealth may be on diverging trajectories, one accumulating toward  $k_H^{ss,c}$  and the other decaying toward the poverty trap.

*Empirical motivation.* Three stylized facts motivate the framework.

*Job polarization and skill obsolescence.* Since the 1990s, labor markets have exhibited pronounced hollowing out (Autor et al., 2003, Goos and Manning, 2007): automation displaces middle-skill tasks, pushing workers into high-skill or low-skill occupations. In our model, this is captured by  $\lambda_{HL}$ —the stochastic destruction of high-productivity matches.

*Rising cost of status.* The real cost of credentials required to access high-productivity occupations has risen faster than inflation (Goldin and Katz, 2008). This maps directly onto an increase in  $\phi$ , which raises  $k^*$ , widens the wait zone, and deepens the trap. Concurrently, skill-biased technological change ( $A_H/A_L$  rising) widens the gap between attractors but also raises the return to signaling—an offsetting force (Brynjolfsson and McAfee, 2014). The unambiguous prediction is that a rising  $\phi$ , holding the productivity gap constant, deepens the poverty trap.

*The low-wealth, high-consumption trap.* Households with positive wealth yet persistently high consumption-to-income ratios and negligible accumulation are documented in the “squeezed middle class” literature (OECD, 2019). Our structurally trapped agents are not liquidity constrained: they possess enough capital to finance  $\phi$  ( $k_L^{ss,c} > \phi$ ), yet signaling is suboptimal because the post-signaling wealth  $k_L^{ss,c} - \phi$  would leave them far below the H-attractor. Their high APC reflects the zero-drift condition, not financial inability to save.

*Plan of the paper.* Section 2 reviews the related literature. Section 3 presents the model. Section 4 characterizes the steady states. Section 5 formulates the optimal control problem. Section 6 derives the coupled HJB system and the Skiba threshold. Section 7 establishes conditions for bimodality. Sections 8–9 describe the numerical method. Section 10 constructs the Kolmogorov Forward Equation. Section 11 presents the calibration. Section 12 reports the results. Section 13 develops the policy implications. Section 14 concludes.

## 2. RELATED LITERATURE

### 2.1. Continuous-Time Heterogeneous Agent Models

Our methodological foundation is the HACT framework of Achdou et al. (2022), extended to aggregate shocks by Ahn et al. (2018), nominal rigidities by Kaplan et al. (2018), and multiple assets by Kaplan and Violante (2014). In these settings, the ergodic wealth distribution is typically unimodal or Pareto-tailed. Our departure is structural: the signaling friction generates an endogenous non-convexity—the Skiba threshold—that produces bifurcation dynamics within an otherwise standard neoclassical environment. No modification of the computational architecture is required beyond the American projection algorithm for the optimal stopping problem.

The economy is formally ergodic, but the mechanism differs from standard diffusion-driven mixing. Ergodicity is guaranteed by the Poisson processes  $\lambda_{LH}$  and  $\lambda_{HL}$ , which create flows between basins even without Brownian diffusion. However, the transition  $L \rightarrow W \rightarrow H$  requires a rare event followed by an accumulation phase during which the opportunity may be lost, producing metastability: the economy is theoretically ergodic but practically polarized on policy-relevant horizons.

## 2.2. *The Signaling Friction*

The economic engine of the model is the labor market signaling mechanism of [Giannini \(2003\)](#), where informational asymmetry between firms and uncredentialed workers generates a pooled wage for the low-skill sector and individual matching for the credentialed. Our continuous-time framework extends this logic along three dimensions: from a binary investment choice to an optimal stopping problem with an endogenous Skiba threshold; from i.i.d. shocks to Brownian diffusion, enabling rigorous characterization of the ergodic distribution via the Kolmogorov Forward Equation (KFE); and from exogenous consumption to intertemporal optimization under CRRA preferences, which delivers the MPC/APC diagnostic. A further innovation is the reversibility of the high-productivity state: unlike [Giannini \(2003\)](#) and [Galor and Zeira \(1993\)](#), where the high state is absorbing, our obsolescence shock generates downward mobility and the Decaying Rentier phenotype.

## 2.3. *Poverty Traps and Persistent Inequality*

The seminal contributions of [Galor and Zeira \(1993\)](#) and [Banerjee and Newman \(1993\)](#) generate persistent stratification through credit market imperfections interacting with indivisible investments. [Buera et al. \(2011\)](#) and [Moll \(2014\)](#) quantify the aggregate TFP losses from the resulting misallocation. Our framework differs in two respects. First, the binding friction is informational and dynamic, not financial: even with unlimited borrowing, the trap persists because the signaling surplus  $D(k)$  incorporates the stochastic duration of the H-regime and the entire future consumption path. Second, the trap is an interior optimum sustained by diminishing returns, not a corner solution sustained by a borrowing limit. This distinction has empirical content: credit-constrained agents respond strongly to windfalls (high MPC), while our trapped agents do not ( $\partial c/\partial k \approx \rho$ ).

The individual production function connects our framework to the misallocation literature. The signaling friction provides a micro-foundation for the distortions studied by [Hsieh and Klenow \(2009\)](#) and [Restuccia and Rogerson \(2008\)](#): agents in the wait zone produce below the frontier not because they lack capital, but because the institutional cost of upgrading exceeds the private return given obsolescence risk.

## 2.4. *Convergence Clubs*

The Twin Peaks phenomenon documented by [Quah \(1996, 1997\)](#) has been explained through threshold externalities ([Azariadis and Drazen, 1990](#)), credit-investment interactions ([Galor and Zeira, 1993](#), [Banerjee and Newman, 1993](#)), and increasing returns. We show that bimodality can arise among ex-ante identical agents without externalities or aggregate non-convexities: the discontinuity is at the individual level (the TFP jump at the signaling threshold), and diminishing returns create two basins whose membership depends on the interaction of wealth and productivity regime. Two agents with identical wealth belong to different clubs if they are in different regimes—a “same-wealth divergence” testable with matched employer-employee data.

## 2.5. *Consumption Heterogeneity*

[Kaplan and Violante \(2014\)](#) distinguish poor and wealthy hand-to-mouth agents, both identified by high MPC. The HANK literature ([Kaplan et al., 2018](#), [Auclert, 2019](#)) builds on this to analyze policy transmission through the MPC distribution. We identify a third phenotype—the

structurally trapped agent—with a distinct signature: low MPC ( $\approx \rho$ ) and high APC ( $\approx 0.90$ ). This agent would be classified as unconstrained by any Euler equation test, yet she is immobile.

Our analysis also connects to the buffer-stock literature (Carroll, 2001): the L-attractor plays an analogous role as a focal point for wealth, but the mechanism is diminishing returns exhaustion rather than the precaution-impatience balance. Finally, unlike present-biased agents (Laibson, 1997, Angeletos et al., 2001) whose high APC reflects self-control failure, our agents' high APC *is* the optimal plan—making commitment devices ineffective and pointing instead to structural reforms ( $\phi$  reduction,  $\lambda_{LH}$  increase).

### 3. THEORETICAL MODEL

We now describe the primitives of the model: preferences, technology, and the regime structure.

ASSUMPTION 1—Preferences and Technology:

(i) Agents have CRRA preferences with risk-aversion parameter  $\gamma > 0$ ,  $\gamma \neq 1$ :

$$u(c) = \frac{c^{1-\gamma}}{1-\gamma}, \quad c > 0.$$

(ii) Time discount rate  $\rho > 0$ .

(iii) Production is Cobb-Douglas with regime-specific total factor productivity (TFP):

$$f_j(k) = A_j k^\alpha, \quad \alpha \in (0, 1), \quad A_j > 0, \quad (1)$$

where  $j \in \{L, H\}$  indexes the productivity regime.

(iv) Capital accumulation with additive noise:

$$dk_t = [f_j(k_t) - c_t - \delta k_t] dt + \sigma dW_t, \quad k_t \geq 0, \quad (2)$$

with depreciation  $\delta \geq 0$  and constant volatility  $\sigma > 0$ .

(v) Reflecting barrier at  $k = 0$ .

REMARK 1—Why Cobb-Douglas rather than linear income: The choice of a concave production function is not merely a functional form assumption—it is essential to the existence of the poverty trap. To see why, consider the deterministic benchmark ( $\sigma = 0$ ,  $\lambda_{LH} = \lambda_{HL} = 0$ ), which isolates the role of the technology.

Under a linear income specification  $y_j(k) = w_j + rk$ , the marginal return to capital  $r$  is constant. The Euler equation  $\dot{c}/c = (r - \delta - \rho)/\gamma$  then has a fixed sign: if  $r - \delta > \rho$ , the agent accumulates without bound; if  $r - \delta < \rho$ , she decumulates to zero. In neither case does a stable interior attractor exist—the economy produces a “bang-bang” outcome, not a trap.

With Cobb-Douglas production, the marginal return  $f'_j(k) = \alpha A_j k^{\alpha-1}$  is a decreasing function of capital. At low  $k$ , returns are high and the agent saves; at high  $k$ , returns are low and she dissaves. The deterministic attractor  $k_j^{ss}$  is the unique capital level where  $f'_j(k) - \delta = \rho$ : the marginal return, net of depreciation, exactly compensates impatience. It is this curvature—not a borrowing constraint, not a non-convexity—that creates the basin of attraction in which agents become trapped.

This deterministic attractor serves as the benchmark throughout the paper. In the full stochastic model, diffusion risk ( $\sigma > 0$ ) and regime switching ( $\lambda_{LH}, \lambda_{HL} > 0$ ) shift the attractor location—producing the coupled attractors  $k_j^{ss,c}$  analyzed in Propositions 6–10—but the fundamental mechanism remains: diminishing returns create the basin, and the signaling friction prevents escape from it.

REMARK 2—Additive noise: The specification  $\sigma dW_t$  (additive) rather than  $\sigma k_t dW_t$  (geometric) ensures that agents face genuine uncertainty at all wealth levels, including  $k \approx 0$  where agents arrive after costly signaling. With Geometric Brownian Motion, diffusion vanishes at  $k = 0$ , eliminating risk precisely where it matters most.

ASSUMPTION 2—Regime structure: There are three states:  $L$  (low productivity),  $W$  (wait—opportunity arrived but not yet exercised), and  $H$  (high productivity, post-signaling).

- (i) In state  $L$ : production  $f_L(k) = A_L k^\alpha$ ; opportunities arrive at Poisson rate  $\lambda_{LH} > 0$ , triggering  $L \rightarrow W$ .
- (ii) In state  $W$ : production  $f_W(k) = A_L k^\alpha$  (unchanged until signaling); the opportunity is lost at Poisson rate  $\lambda_{HL} > 0$ , triggering  $W \rightarrow L$ .
- (iii) The agent in  $W$  may *signal* at any chosen time  $\tau$  by paying a lump-sum cost  $\phi > 0$  in capital, transitioning to state  $H$  at wealth  $k_\tau - \phi$ .
- (iv) In state  $H$ : production  $f_H(k) = A_H k^\alpha$  with  $A_H > A_L$ ; productivity is lost at Poisson rate  $\lambda_{HL}$ , triggering  $H \rightarrow L$ .

REMARK 3—Common obsolescence rate: The loss of the signaling opportunity in state  $W$  and the productivity reversion in state  $H$  are both governed by the rate  $\lambda_{HL}$ . This reflects a common source of technological turbulence: the same structural forces that erode an established credential also close the window for acquiring a new one. This parsimony can be relaxed by introducing a separate rate  $\lambda_{WL}$  without affecting the qualitative results.

ASSUMPTION 3—Parameter restrictions:

- (i)  $A_H > A_L > 0$  (signaling leads to higher TFP).
- (ii)  $\phi > 0$  (signaling is costly).
- (iii)  $\delta > 0$  (capital depreciates).

#### 4. STEADY STATES FROM DIMINISHING RETURNS

The key advantage of Cobb-Douglas production is that stable interior attractors arise naturally from diminishing returns, without requiring delicate parameter restrictions.

##### 4.1. Deterministic Steady States

PROPOSITION 4—Deterministic steady states: *When  $\sigma = 0$  and  $\lambda_{LH} = \lambda_{HL} = 0$ , each regime  $j$  is an independent Ramsey problem with production  $f_j(k) = A_j k^\alpha$ . The unique stable steady state is:*

$$k_j^{ss} = \left( \frac{\alpha A_j}{\rho + \delta} \right)^{1/(1-\alpha)}, \quad j \in \{L, H\}. \quad (3)$$

*This is the capital level where the net marginal return equals the discount rate:*

$$f'_j(k_j^{ss}) - \delta = \alpha A_j (k_j^{ss})^{\alpha-1} - \delta = \rho. \quad (4)$$

PROOF: The deterministic Euler equation for the Ramsey problem with  $f_j(k) = A_j k^\alpha$  is:

$$\frac{\dot{c}}{c} = \frac{1}{\gamma} [f'_j(k) - \delta - \rho] = \frac{1}{\gamma} [\alpha A_j k^{\alpha-1} - \delta - \rho].$$

At steady state  $\dot{c} = 0$ , so  $\alpha A_j (k_j^{ss})^{\alpha-1} = \rho + \delta$ , giving (3). Stability follows because  $f_j''(k) < 0$ : for  $k < k_j^{ss}$ , the marginal return exceeds  $\rho + \delta$ , so consumption grows and drift is positive; for  $k > k_j^{ss}$ , the reverse holds. ■

REMARK 5—Separation from TFP gap: The ratio of steady states is:

$$\frac{k_H^{ss}}{k_L^{ss}} = \left( \frac{A_H}{A_L} \right)^{1/(1-\alpha)}.$$

The skill gap directly controls the separation between the two modes of the wealth distribution.

#### 4.2. Stochastic Steady States

PROPOSITION 6—Stochastic steady states: *With additive noise  $\sigma > 0$  and no switching ( $\lambda_{LH} = \lambda_{HL} = 0$ ), the stochastic steady state in regime  $j$  satisfies:*

$$f_j'(k_j^{ss}(\sigma)) - \delta = \rho - \underbrace{\frac{1}{2} \gamma(\gamma + 1) \sigma^2 \frac{c_j''}{c_j} \Big|_{k_j^{ss}(\sigma)}}_{\equiv \Pi_j(\sigma) > 0}, \quad (5)$$

where  $\Pi_j(\sigma)$  is the precautionary correction. Since  $\Pi_j > 0$ , the net marginal return at the stochastic attractor is strictly below  $\rho$ :

$$f_j'(k_j^{ss}(\sigma)) - \delta < \rho = f_j'(k_j^{ss}(0)) - \delta.$$

By strict concavity of  $f_j$  ( $f_j'' < 0$ ), this implies  $k_j^{ss}(\sigma) > k_j^{ss}(0)$ . The correction  $\Pi_j(\sigma)$  is bounded and vanishes as  $\sigma \rightarrow 0$ , so that  $k_j^{ss}(\sigma) \rightarrow k_j^{ss}(0)$  continuously.

PROOF SKETCH: At the stochastic steady state,  $\dot{c}_j = 0$  and  $\mu_j = 0$ . Setting the Euler equation (Proposition 25) to zero in the uncoupled case yields (5). Under CRRA preferences with  $\gamma > 0$ , the prudence coefficient  $\gamma + 1$  is strictly positive, and with additive noise the term  $c_j''/c_j$  is negative at the attractor (the consumption function is locally concave in  $k$ ), making  $\Pi_j > 0$ . Since additive noise does not scale with  $k$ , the precautionary correction remains bounded as  $k$  varies. The exact value of  $k_j^{ss}(\sigma)$  depends on the global shape of  $c_j(k)$  and is determined numerically. ■

REMARK 7—Economic interpretation: The precautionary motive shifts the attractor upward because agents exposed to wealth risk save more as a buffer. Under additive noise, this buffer is independent of the wealth level (unlike geometric noise, where the buffer would scale with  $k$ ). The upward shift is quantitatively modest under our calibration but conceptually important: it widens the gap between  $k_L^{ss}(\sigma)$  and the borrowing constraint, confirming that structurally trapped agents are not near  $k = 0$ .

#### 4.3. Full Model: Coupling Effects

We now analyze how regime switching ( $\lambda_{LH}, \lambda_{HL} > 0$ ) modifies the attractors relative to the uncoupled benchmarks of Proposition 6. Let  $k_j^{ss,u} \equiv k_j^{ss}(\sigma)$  denote the stochastic attractor of regime  $j$  solved in isolation, and  $k_j^{ss,c}$  the attractor under the full coupled system, i.e. when  $\lambda_{LH}, \lambda_{HL}, \sigma > 0$ .

PROPOSITION 8—Upward shift of the L-attractor: Let  $\sigma > 0$  and  $\lambda_{LH} > 0$ . Suppose the L-attractor lies below the Skiba threshold:  $k_L^{ss,c} < k^*$ . Then:

$$k_L^{ss,c} > k_L^{ss,u}. \quad (6)$$

PROOF: At the uncoupled attractor  $k_L^{ss,u}$ , the Euler equation with  $\dot{c}_L = 0$  and  $\lambda_{LH} = 0$  yields (Proposition 6):

$$f'_L(k_L^{ss,u}) - \delta = \rho - \Pi_L(k_L^{ss,u}), \quad (7)$$

where  $\Pi_L > 0$  is the precautionary correction.

At the coupled attractor  $k_L^{ss,c}$ , the full Euler equation (Proposition 25) with  $\dot{c}_L = 0$  gives:

$$f'_L(k_L^{ss,c}) - \delta = \rho - \Pi_L(k_L^{ss,c}) + \lambda_{LH} \left( 1 - \frac{u'(c_W(k_L^{ss,c}))}{u'(c_L(k_L^{ss,c}))} \right). \quad (8)$$

We show the switching term is strictly negative. The key observation is that the W-agent at  $k = k_L^{ss,c}$  produces with the *same* technology  $f_L$  as the L-agent—she has received a signaling opportunity but has not yet exercised it. However, the two agents have different saving behavior at the same wealth. The L-agent is at her zero-drift steady state:  $\mu_L(k_L^{ss,c}) = 0$ , so  $c_L(k_L^{ss,c}) = f_L(k_L^{ss,c}) - \delta k_L^{ss,c}$ . The W-agent, by contrast, is accumulating toward the Skiba threshold  $k^*$ : since  $k_L^{ss,c} < k^*$  by assumption, signaling is not yet optimal ( $D(k_L^{ss,c}) > 0$ ), and the W-agent saves in order to reach the exercise boundary. Her drift is therefore strictly positive:

$$\mu_W(k_L^{ss,c}) = f_L(k_L^{ss,c}) - \delta k_L^{ss,c} - c_W(k_L^{ss,c}) > 0 = \mu_L(k_L^{ss,c}).$$

Since both agents face the same net income  $f_L(k_L^{ss,c}) - \delta k_L^{ss,c}$ , the positive drift of the W-agent directly implies:

$$c_W(k_L^{ss,c}) < c_L(k_L^{ss,c}). \quad (9)$$

By strict concavity of  $u$ , this yields  $u'(c_W(k_L^{ss,c})) > u'(c_L(k_L^{ss,c}))$ , so:

$$\lambda_{LH} \left( 1 - \frac{u'(c_W)}{u'(c_L)} \right) < 0.$$

Substituting into (8) and holding the precautionary term fixed at  $\Pi_L(k_L^{ss,c})$ :

$$f'_L(k_L^{ss,c}) - \delta < \rho - \Pi_L(k_L^{ss,c}). \quad (10)$$

To compare with (7), we note that the precautionary correction  $\Pi_L(k) = \frac{1}{2}\gamma(\gamma+1)\sigma^2 c''_L(k)/c_L(k)$  depends on the local curvature of the consumption function. Under the maintained assumption that  $\Pi_L$  does not decrease between  $k_L^{ss,u}$  and  $k_L^{ss,c}$ —which holds when the consumption function does not become substantially more convex over this range—inequality (10) implies  $f'_L(k_L^{ss,c}) < f'_L(k_L^{ss,u})$ . By the strict concavity of  $f_L$  ( $f''_L < 0$ ), we conclude  $k_L^{ss,c} > k_L^{ss,u}$ . ■

REMARK 9—Economic interpretation: The L-agent in the coupled system saves more than in isolation because the possibility of a future signaling opportunity raises the shadow value of wealth. An agent in state L cannot signal—she must first receive the opportunity (at rate  $\lambda_{LH}$ ). But she *anticipates* that, upon arrival, she will transition to the W-state where every additional unit of capital brings her closer to the Skiba threshold  $k^*$  and thus to the high-productivity regime. This expected gain from being wealthier at the moment of transition reduces current

consumption and pushes the L-attractor upward. The effect is stronger when  $\lambda_{LH}$  is larger (opportunities more frequent) or when the wait zone  $[\phi, k^*)$  is narrower (less accumulation needed to reach  $k^*$ ).

We now turn to the H-attractor. The analysis is more delicate than for the L-attractor, because the coupling introduces effects that operate in opposite directions.

**PROPOSITION 10**—Effects on the H-attractor: *Let  $\sigma > 0$  and  $\lambda_{HL} > 0$ . At the coupled H-attractor  $k_H^{ss,c}$ , the Euler equation with  $\dot{c}_H = 0$  yields:*

$$f'_H(k_H^{ss,c}) - \delta = \rho - \Pi_H(k_H^{ss,c}) + \lambda_{HL} \left( 1 - \frac{u'(c_L(k_H^{ss,c}))}{u'(c_H(k_H^{ss,c}))} \right). \quad (11)$$

*If  $c_H(k_H^{ss,c}) > c_L(k_H^{ss,c})$ —which holds when  $k_H^{ss,c}$  is sufficiently above  $k_L^{ss,c}$ , so that the H-agent's higher income dominates the L-agent's dissaving at that capital level—then the switching term is strictly negative. This has two economic interpretations:*

- (i) **Precautionary saving against regime loss.** *The agent faces the risk of losing  $A_H$ . Under prudence ( $\gamma > 0$ ), she accumulates a buffer to cushion the income drop upon reverting to  $A_L$ .*
- (ii) **Consumption smoothing across regimes.** *The agent internalizes the consumption drop  $c_H \rightarrow c_L$  that accompanies the regime switch. To reduce this gap, she consumes less in H and saves more.*

*Both effects, evaluated at the steady-state Euler equation, push  $k_H^{ss,c}$  upward relative to the deterministic benchmark  $k_H^{ss}(0)$ .*

*However, the coupling also modifies the H-agent's problem globally. The prospect of future reversion to  $A_L$  reduces the present value of the H-regime, reshaping the value function  $V_H$  and the consumption policy  $c_H(k)$  at every capital level—not only at the attractor. This “front-loading” channel raises  $c_H(k)$  for a given  $k$ , which, taken alone, would push the attractor downward. The net direction of the shift relative to the uncoupled stochastic benchmark  $k_H^{ss,u}$  depends on the relative strength of these channels and is parameter-dependent.*

**REMARK 11**—Direction of the shift under the baseline calibration: The Euler equation analysis identifies forces that push  $k_H^{ss,c}$  both upward (precautionary saving, consumption smoothing) and downward (front-loading of consumption). Under our baseline calibration, the numerical results confirm that the upward forces dominate in aggregate: the full-model attractor  $k_H^{ss,c} = 16.12$  lies well above the deterministic benchmark  $k_H^{ss}(0) = 14.12$ . Determining the sign of the shift relative to the uncoupled stochastic attractor  $k_H^{ss,u}$  would require solving the H-regime in isolation with  $\sigma > 0$  and  $\lambda_{HL} = 0$ ; we leave this decomposition for future work.

**PROPOSITION 12**—Attractor gap under coupling: *Under the baseline calibration (Table I), the coupled attractors are  $k_L^{ss,c} = 11.50$  and  $k_H^{ss,c} = 16.12$ , yielding a gap of 4.62. Both lie above their deterministic counterparts ( $k_L^{ss}(0) = 10.12$ ,  $k_H^{ss}(0) = 14.12$ , gap = 4.00). The modest widening of the gap (4.62 vs. 4.00) indicates that the precautionary motive shifts both attractors upward, with the H-attractor rising slightly more in absolute terms.*

**REMARK 13**—Sufficient separation for bimodality: For the stationary distribution to be bimodal, the attractor gap must be large relative to the local dispersion at each mode:

$$k_H^{ss,c} - k_L^{ss,c} \gg \sigma_L^{ss} + \sigma_H^{ss},$$

where  $\sigma_j^{ss}$  is the stationary standard deviation near attractor  $j$ . When this separation condition fails, the two modes merge into a single peak. Section 7 provides a formal statement.

## 5. THE OPTIMAL CONTROL PROBLEM

Before deriving the Hamilton–Jacobi–Bellman equations, we state the agent’s problem in its primitive form. Each agent chooses a consumption plan  $\{c_t\}_{t \geq 0}$  to maximize expected lifetime utility, subject to the stochastic law of motion for capital, the regime structure, and non-negativity constraints.

DEFINITION 14—The agent’s problem: Given an initial capital stock  $k_0 > 0$  and an initial regime  $s_0 \in \{L, W, H\}$ , the agent solves:

$$\sup_{\{c_t\}_{t \geq 0}, \tau} \mathbb{E}_0 \left[ \int_0^\infty e^{-\rho t} u(c_t) dt \right], \quad (12)$$

where  $u(c) = c^{1-\gamma}/(1-\gamma)$  with  $\gamma > 0$ ,  $\gamma \neq 1$ . The stopping time  $\tau$  does not appear in the integrand: the signaling cost  $\phi$  is paid in capital, not in utility. The decision  $\tau$  affects the objective indirectly, by altering the capital trajectory (13) and hence the feasible consumption paths from  $\tau$  onward. The objective function is subject to:

(i) *State equation.* Capital evolves according to:

$$dk_t = [f_{s_t}(k_t) - c_t - \delta k_t] dt + \sigma dW_t, \quad (13)$$

where  $f_{s_t}(k) = A_{s_t} k^\alpha$  is the production function in the current regime  $s_t$ ,  $\delta \geq 0$  is the depreciation rate,  $\sigma > 0$  is the diffusion coefficient, and  $W_t$  is a standard Brownian motion.

(ii) *Regime transitions.* The regime  $s_t$  evolves on  $\{L, W, H\}$  through a combination of exogenous Poisson events and one endogenous decision:

$$L \rightarrow W \quad \text{at Poisson rate } \lambda_{LH} \quad (\text{signaling opportunity arrives}), \quad (14)$$

$$W \rightarrow H \quad \text{at stopping time } \tau \text{ chosen by the agent, with cost } \phi \quad (\text{opportunity exercised}), \quad (15)$$

$$\{W, H\} \rightarrow L \quad \text{at Poisson rate } \lambda_{HL} \quad (\text{obsolescence shock}). \quad (16)$$

(ii-bis) *Production in the W-state.* In state W, production remains  $A_L k^\alpha$ ; the W-state differs from L only in that the agent holds the option to signal.

(iii) *Initial condition.*

$$k_0 > 0 \quad \text{given}, \quad s_0 \in \{L, W, H\} \quad \text{given}. \quad (17)$$

(iv) *Non-negativity constraints.*

$$c_t \geq 0, \quad k_t \geq 0, \quad f_{s_t}(k_t) = A_{s_t} k_t^\alpha \geq 0 \quad \text{for all } t \geq 0. \quad (18)$$

The constraint  $k_t \geq 0$  is enforced by a reflecting barrier at  $k = 0$  (Assumption 1(v)). The constraint  $f_{s_t}(k_t) \geq 0$  is automatically satisfied by the Cobb-Douglas specification with  $A_j > 0$  and  $k_t \geq 0$ .

(v) *Transversality condition.*

$$\lim_{t \rightarrow \infty} \mathbb{E}_0 [e^{-\rho t} V_{s_t}(k_t)] = 0, \quad (19)$$

where  $V_j(k)$  is the value function in regime  $j$ . This condition rules out Ponzi schemes and ensures that the agent does not indefinitely postpone consumption.

(vi) *Signaling feasibility*. The stopping time  $\tau$  is admissible only if:

$$k_{\tau-} \geq \phi, \quad (20)$$

so that post-signaling capital  $k_{\tau+} = k_{\tau-} - \phi \geq 0$ . If the agent is in state  $W$  with  $k_t < \phi$ , signaling is not feasible and the agent must either accumulate further or let the opportunity expire.

REMARK 15—Two control variables: The agent's problem has two control variables: the consumption flow  $c_t \geq 0$  (chosen continuously in all states) and the stopping time  $\tau$  (chosen only in state  $W$ ). The consumption choice is a standard continuous control; the signaling decision is a singular control of impulse type—a discrete action (pay  $\phi$ , change regime) taken at an endogenously chosen instant. The coexistence of these two control types is what gives the problem its American option structure: the  $W$ -agent continuously optimizes consumption while simultaneously deciding whether to exercise the signaling option.

REMARK 16—Well-posedness: The objective (12) is well-defined under Assumptions 1–3. The CRRA utility function with  $\gamma > 0$  ensures  $u(c) < \infty$  for all  $c > 0$ , and the Cobb-Douglas production function with  $\alpha \in (0, 1)$  bounds income growth, so that the integral converges under the transversality condition (19). The reflecting barrier at  $k = 0$  ensures  $k_t \geq 0$  almost surely, and the additive noise specification guarantees that  $k_t$  does not explode in finite time.

The value functions associated with problem (12)–(20) satisfy a system of Hamilton–Jacobi–Bellman equations, which we derive in the next section.

## 6. HAMILTON–JACOBI–BELLMAN EQUATIONS

### 6.1. The HJB System

Let  $V_L(k)$ ,  $V_W(k)$ , and  $V_H(k)$  denote the value functions in states  $L$ ,  $W$ , and  $H$ . Define the drift and differential operator for state  $j$ :

$$\mu_j(k) = f_j(k) - c - \delta k, \quad \mathcal{A}_j V = \mu_j(k) V' + \frac{1}{2} \sigma^2 V'',$$

where the optimal consumption satisfies  $c = (V')^{-1/\gamma}$  from the first-order condition  $u'(c) = V'(k)$ .

DEFINITION 17—Value of holding the opportunity:

$$V_{H_0}(k) = \begin{cases} \max(V_W(k), V_H(k - \phi)) & \text{if } k \geq \phi, \\ V_W(k) & \text{if } k < \phi. \end{cases} \quad (21)$$

The HJB system is:

**State  $L$  (no opportunity):**

$$\rho V_L = \max_{c>0} \left\{ u(c) + (A_L k^\alpha - c - \delta k) V_L' + \frac{1}{2} \sigma^2 V_L'' \right\} + \lambda_{LH} (V_{H_0} - V_L). \quad (22)$$

**State H (high TFP):**

$$\rho V_H = \max_{c>0} \left\{ u(c) + (A_H k^\alpha - c - \delta k) V_H' + \frac{1}{2} \sigma^2 V_H'' \right\} + \lambda_{HL} (V_L - V_H). \quad (23)$$

**State W (variational inequality):**

The W-agent faces a problem that is qualitatively different from the L- and H-agents. At each instant, she must decide whether to continue waiting (accumulating capital at productivity  $A_L$  while the option remains alive) or to signal immediately (paying  $\phi$  and jumping to state H). This “continue or exercise” decision generates a variational inequality rather than a standard HJB equation.

To see why, consider two possibilities at each wealth level  $k \geq \phi$ . If the agent finds it optimal to *wait*, the value function  $V_W(k)$  satisfies the standard HJB equation—the same equation she would solve if signaling were not available—augmented by the risk of losing the opportunity at rate  $\lambda_{HL}$ :

$$\rho V_W = \max_{c>0} \left\{ u(c) + (A_L k^\alpha - c - \delta k) V_W' + \frac{1}{2} \sigma^2 V_W'' \right\} + \lambda_{HL} (V_L - V_W).$$

If instead it is optimal to *signal immediately*, the value of being in state W must equal the value of being in state H at post-signaling wealth:

$$V_W(k) = V_H(k - \phi).$$

At any given  $k$ , exactly one of these conditions holds with equality while the other holds as an inequality. In the *wait region* ( $k < k^*$ ), the HJB equation binds and  $V_W(k) > V_H(k - \phi)$ : the surplus of waiting exceeds the value of immediate exercise, because the post-signaling wealth  $k - \phi$  would leave the agent too far below the H-attractor. In the *signal region* ( $k \geq k^*$ ), the value-matching condition binds and the HJB residual is strictly positive: continuing to wait would be suboptimal, as the option is sufficiently deep in the money that immediate exercise dominates. The two conditions are compactly expressed as:

$$\min \left( \underbrace{\rho V_W - \max_{c>0} \left\{ u(c) + (A_L k^\alpha - c - \delta k) V_W' + \frac{1}{2} \sigma^2 V_W'' \right\} - \lambda_{HL} (V_L - V_W)}_{= 0 \text{ in the wait region}}, \underbrace{V_W - V_H(k - \phi)}_{= 0 \text{ in the signal region}} \right) = 0. \quad (24)$$

for  $k \geq \phi$ , and the standard HJB (without the signaling option) for  $k < \phi$  where signaling is not feasible.

The min operator encodes the logic of optimal stopping: at each  $k$ , the agent selects the action that yields the *higher* value. If waiting is better ( $V_W(k) > V_H(k - \phi)$ ), the value-matching term is strictly positive while the HJB residual is zero; if signaling is better, the value-matching term is zero while the HJB residual is non-negative. The min of the two expressions equals zero in both cases, and is strictly positive in neither—this is the complementary slackness structure characteristic of variational inequalities.

REMARK 18—Smooth pasting and the need for viscosity solutions: The boundary between the wait and signal regions is the Skiba threshold  $k^*$ : the lowest wealth level at which immediate signaling is optimal. Unlike the classical Skiba problem—where an agent chooses once between two permanent trajectories and the value function may exhibit a kink—here the agent faces a continuous optimal stopping problem with diffusion ( $\sigma > 0$ ). The Brownian noise allows the agent to adjust the exercise boundary with arbitrary precision, which generically imposes *smooth pasting* at  $k^*$ :

$$V'_W(k^*) = V'_H(k^* - \phi). \quad (25)$$

The value function  $V_W$  is therefore  $C^1$  at  $k^*$ : continuous with a continuous first derivative. However, the *second* derivative  $V''_W$  is generally discontinuous at  $k^*$ : in the wait region,  $V''_W$  is governed by the HJB equation under technology  $A_L$ , while in the signal region,  $V''_W(k) = V''_H(k - \phi)$ , which is governed by  $A_H$ . Since  $A_H \neq A_L$ , these curvatures generically differ at the boundary. By the first-order condition  $u'(c_W) = V'_W$ , smooth pasting ensures that the consumption policy  $c_W(k)$  is *continuous* at  $k^*$ . But differentiating yields  $c'_W(k) = V''_W(k)/u''(c_W(k))$ , so the jump in  $V''_W$  produces a kink in  $c_W$ : consumption is continuous but its slope changes abruptly at the exercise boundary. This failure of  $C^2$  regularity at  $k^*$ —not a kink in the value function—is what renders the classical smooth solution concept inapplicable and motivates the use of viscosity solutions.

REMARK 19—Viscosity solutions: The failure of  $C^2$  regularity at  $k^*$  is not merely a technical nuisance but a structural feature of any model with an embedded optimal stopping problem. Although smooth pasting ensures that  $V_W$  is  $C^1$  at the exercise boundary, the discontinuity in  $V''_W$  means that the HJB equation (24)—which involves the second derivative through the diffusion term  $\frac{1}{2}\sigma^2 V''_W$ —cannot be evaluated classically at  $k^*$ . To handle this rigorously, we adopt the viscosity solution framework of [Crandall and Lions \(1983\)](#), extended to stochastic control problems by [Fleming and Soner \(2006\)](#) and applied to heterogeneous agent models by [Achdou et al. \(2022\)](#). A viscosity solution of (24) satisfies the variational inequality in a weak sense: at points where  $V''_W$  does not exist, the equation is required to hold for all smooth test functions that touch the value function from above (viscosity subsolution) and from below (viscosity supersolution), rather than requiring classical differentiability of  $V_W$  itself. The upwind finite difference scheme of Section 8—which selects forward or backward differences according to the sign of the drift—converges to the viscosity solution as  $\Delta k \rightarrow 0$ , providing a numerically robust treatment of the non-differentiability without requiring *ad hoc* smoothing.

## 6.2. Signaling Surplus and Skiba Threshold

DEFINITION 20—Signaling surplus: For an agent in state  $W$  with capital  $k \geq \phi$ , the signaling surplus is:

$$D(k) = V_W(k) - V_H(k - \phi), \quad k \geq \phi. \quad (26)$$

DEFINITION 21—Skiba threshold: The Skiba threshold is the lowest wealth level at which immediate signaling is optimal:

$$k^* = \inf\{k \geq \phi : D(k) = 0\}. \quad (27)$$

For  $k < k^*$ , the surplus of waiting is strictly positive ( $D(k) > 0$ ) and the agent holds the option. For  $k \geq k^*$ , the agent signals immediately upon opportunity arrival, so that  $V_W(k) = V_H(k - \phi)$  and  $D(k) = 0$ .

REMARK 22—Three cases: Depending on the parameters, three configurations arise:

- (a) *Interior threshold* ( $k^* \in (\phi, \infty)$ ): signaling is feasible at  $k = \phi$  but not optimal; the agent waits until  $k = k^* > \phi$ . This is the generic case under our calibration and the source of the “Frustrated Aspirants” phenotype.
- (b) *Immediate signaling* ( $k^* = \phi$ ): the agent signals as soon as signaling is affordable. This arises when  $A_H/A_L$  is sufficiently large or  $\lambda_{HL}$  is sufficiently small that  $D(\phi) = 0$ : the productivity gain from switching is so large, or the expected duration of the H-regime so long, that even the minimal post-signaling wealth  $k - \phi \approx 0$  justifies immediate exercise. The wait zone vanishes and all W-agents signal at the first feasible instant.
- (c) *No signaling* ( $k^* = +\infty$ ):  $D(k) > 0$  for all  $k \geq \phi$ . The obsolescence risk is so severe, or the productivity gap so narrow, that the expected benefit of signaling never exceeds the cost. No agent transitions to H, the H-density is identically zero, and the economy effectively reduces to a single-attractor model at  $A_L$ .

### 6.3. Properties of the Value Functions

PROPOSITION 23—Concavity: *The value functions  $V_L$ ,  $V_W$ ,  $V_H$  are strictly concave on  $(0, \infty)$ .*

PROOF: See Appendix 15.1 ■

PROPOSITION 24—Value ordering:

- (i)  $V_H(k) > V_W(k) > V_L(k)$  for all  $k > 0$ .
- (ii)  $V_W(k) \geq V_H(k - \phi)$  for  $k \geq \phi$ , with equality if and only if  $k \geq k^*$ .
- (iii) *The full ordering is therefore:*

$$V_H(k) > V_W(k) \geq V_H(k - \phi) \quad \text{for } k \geq \phi.$$

PROOF: See Appendix 15.2 ■

### 6.4. Euler Equations

We derive the consumption Euler equation by differentiating the first-order condition along the optimal path. The derivation proceeds in three steps: extract the first-order condition from the HJB, apply Itô’s lemma to the co-state variable, and eliminate the value function derivatives using the envelope condition.

PROPOSITION 25—Euler equations: *The optimal consumption in state  $j \in \{L, H\}$  satisfies:*

$$\frac{\dot{c}_j}{c_j} = \frac{1}{\gamma} \left[ \underbrace{f'_j(k) - \delta - \rho + \frac{1}{2}\gamma(\gamma+1)\sigma^2 \frac{c'_j}{c_j}}_{\text{precautionary}} - \underbrace{\lambda_{\text{out},j} \left( 1 - \frac{u'(c_{\text{other}})}{u'(c_j)} \right)}_{\text{regime switching}} \right], \quad (28)$$

where  $\lambda_{\text{out},j}$  is the outgoing Poisson rate from state  $j$  (i.e.,  $\lambda_{\text{out},L} = \lambda_{LH}$  and  $\lambda_{\text{out},H} = \lambda_{HL}$ ), and  $c_{\text{other}}$  is the consumption in the destination state evaluated at the same capital  $k$ .

PROOF: See Appendix 15.3 ■

REMARK 26—Interpretation of each term: The Euler equation (28) decomposes the consumption growth rate into three components:

- (i) *The standard Ramsey term*  $(f'_j(k) - \delta - \rho)/\gamma$ . When the net marginal return to capital exceeds the discount rate, consumption is growing (the agent is accumulating); when it falls below  $\rho$ , consumption is declining (decumulation). In the deterministic uncoupled benchmark ( $\sigma = 0$ ,  $\lambda_{\text{out},j} = 0$ ), this is the only term, and the steady state satisfies  $f'_j(k_j^{\text{ss}}) = \rho + \delta$ .
- (ii) *The precautionary term*  $\frac{1}{2}(\gamma + 1)\sigma^2 c''_j/c_j$ . This arises from the convexity of marginal utility ( $u''' > 0$  under CRRA with  $\gamma > 0$ , since the coefficient of absolute prudence is  $-u'''/u'' = (\gamma + 1)/c > 0$ ). The term  $c''_j/c_j$  captures the local curvature of the consumption policy: when the consumption function is concave in  $k$  ( $c'_j < 0$ ), the precautionary term is negative, meaning it *reduces* the required rate of return for the agent to be willing to hold capital. This induces additional saving, shifting the attractor upward (Proposition 6).
- (iii) *The regime-switching term*  $-\lambda_{\text{out},j}(1 - u'(c_{\text{other}})/u'(c_j))/\gamma$ . This captures the agent's anticipation of a regime change. If  $c_{\text{other}} < c_j$  at the current  $k$  (the destination state has lower consumption), then  $u'(c_{\text{other}}) > u'(c_j)$ , the ratio exceeds unity, and the term is negative: the anticipated consumption drop lowers the effective discount rate, inducing the agent to save more. Conversely, if  $c_{\text{other}} > c_j$ , the agent anticipates higher future consumption and saves less. For the L-agent,  $c_{\text{other}} = c_W < c_L$  at  $k_L^{\text{ss},c}$  (equation (9) in the proof of Proposition 8), so the switching term reinforces precautionary saving.

REMARK 27—Steady-state characterization: At the stochastic steady state  $\dot{c}_j = 0$ , equation (48) yields:

$$f'_j(k_j^{\text{ss}}) - \delta = \rho - \frac{1}{2}\gamma(\gamma + 1)\sigma^2 \frac{c''_j}{c_j} \Big|_{k_j^{\text{ss}}} + \lambda_{\text{out},j} \left( 1 - \frac{u'(c_{\text{other}}(k_j^{\text{ss}}))}{u'(c_j(k_j^{\text{ss}}))} \right).$$

The net marginal return to capital at the attractor differs from  $\rho$  by the precautionary and switching corrections. This is the equation used in Propositions 6 and 8 to characterize the uncoupled and coupled attractors, respectively.

### 6.5. Boundary Conditions

The HJB system (22)–(24) requires boundary conditions at both ends of the capital domain  $[0, k_{\text{max}}]$ . We derive these from the primitives of the model—the reflecting barrier (Assumption 1(v)) and the transversality condition (19)—and then state their numerical implementation.

PROPOSITION 28—Lower boundary: reflecting barrier: *At  $k = 0$ , the reflecting barrier (Assumption 1(v)) imposes a Neumann-type condition on the HJB system: the backward advection term vanishes, so that no mass flows to  $k < 0$ . The value function  $V_j$  satisfies the HJB equation at  $k = 0$  with the slope  $V'_j(0)$  determined endogenously by the equation itself. In particular:*

- (a)  *$V'_j(0)$  is finite but large: since  $f'_j(k) = \alpha A_j k^{\alpha-1} \rightarrow \infty$  as  $k \rightarrow 0$ , the marginal value of capital near the origin is high, reflecting the strong returns available at low wealth levels.*
- (b) *The drift at the origin is non-negative:  $\mu_j(0, c_j(0)) \geq 0$ . Since  $f_j(0) = 0$ , the agent at  $k = 0$  has zero income and consumes  $c_j(0) = 0$ ; the only source of inward movement is the diffusion term  $\sigma dW_t$ , and the reflecting barrier prevents outward leakage.*

*The corresponding condition for the stationary distribution—the zero-flux condition on the probability current  $J_j(0) = 0$ —is derived in Section 15.5.2.*

PROOF: The reflecting barrier is a standard construction for diffusion processes on  $[0, \infty)$ : when the process  $k_t$  reaches zero, an instantaneous upward push  $dL_t$  (the local time at

zero) prevents  $k_t$  from becoming negative. In the HJB framework, this is implemented via a Neumann-type condition: the generator  $\mathcal{L}_j$  does not require backward advection at  $k = 0$  (there is no mass flow to  $k < 0$ ). The slope  $V_j'(0)$  is not a free parameter but is determined by the HJB equation evaluated at  $k = 0$ :

$$\rho V_j(0) = u(c_j(0)) + \mu_j(0, c_j(0)) V_j'(0) + \frac{1}{2} \sigma^2 V_j''(0) + \lambda_{\text{out},j} (V_{\text{other}}(0) - V_j(0)),$$

with  $c_j(0) = (V_j'(0))^{-1/\gamma}$  from the first-order condition. This is a single equation in the unknowns  $V_j(0)$ ,  $V_j'(0)$ , and  $V_j''(0)$ , which is closed by the global solution of the HJB system. ■

PROPOSITION 29—Upper boundary: transversality: *The transversality condition (19),*

$$\lim_{t \rightarrow \infty} \mathbb{E}_0 [e^{-\rho t} V_{s_t}(k_t)] = 0,$$

*rules out explosive paths and, for a sufficiently large  $k_{\max}$ , implies the following condition at the upper boundary: the agent at  $k_{\max}$  consumes her entire net income,*

$$c_j(k_{\max}) = f_j(k_{\max}) - \delta k_{\max}, \quad (29)$$

*so that  $\mu_j(k_{\max}) = 0$  (zero drift).*

PROOF: Under Cobb-Douglas production with  $\alpha < 1$ , the marginal return  $f_j'(k) = \alpha A_j k^{\alpha-1}$  is strictly decreasing and satisfies  $f_j'(k) \rightarrow 0$  as  $k \rightarrow \infty$ . For  $k$  sufficiently large,  $f_j'(k) - \delta < \rho$ : the net marginal return falls below the discount rate. In this region, the Euler equation (48) with  $f_j'(k) - \delta < \rho$  implies  $\dot{c}_j/c_j < 0$  (absent dominant precautionary or switching corrections): consumption is declining and the agent is decumulating.

A path along which  $k_t \rightarrow \infty$  would require  $\mu_j > 0$  indefinitely, which in turn requires  $c_j < f_j(k) - \delta k$ . But for large  $k$ , this implies the agent under-consumes relative to her income despite  $f_j'(k) < \rho + \delta$ —a violation of the Euler equation. More precisely, such a path generates  $V_j(k_t) \sim O(k_t^{1-\gamma})$  for  $\gamma < 1$  (or  $V_j(k_t) \sim O(\ln k_t)$  for  $\gamma = 1$ ), and the discount factor  $e^{-\rho t}$  does not decay fast enough to drive  $e^{-\rho t} V_{s_t}(k_t)$  to zero, violating transversality.

The zero-drift condition (29) is therefore the natural boundary condition at  $k_{\max}$ : it ensures that  $k_{\max}$  acts as an absorbing-like boundary from which the agent neither accumulates nor decumulates (ignoring diffusion), consistent with the transversality requirement that no value is “left at infinity.” ■

REMARK 30—Choice of  $k_{\max}$ : The upper boundary  $k_{\max}$  is a computational parameter, not a feature of the model. It must be chosen large enough that  $f_H'(k_{\max}) - \delta < \rho$  (so that even the high-productivity agent is in the decumulation region) and that the stationary distribution places negligible mass near  $k_{\max}$ .

REMARK 31—Numerical implementation: In the finite difference scheme of Section 8, the boundary conditions are implemented as follows:

- (a) *Lower boundary* ( $i = 1$ ,  $k_1 = \varepsilon$ ): the backward difference coefficient is set to  $y_1 = 0$ , ensuring no backward advection (no mass flows below  $k_1$ ). This is the discrete analogue of the zero-flux condition.
- (b) *Upper boundary* ( $i = N$ ,  $k_N = k_{\max}$ ): the forward difference coefficient is set to  $x_N = 0$ , and the consumption policy is fixed at  $c_j(k_N) = f_j(k_N) - \delta k_N$ , imposing zero drift. This ensures that the scheme does not require values outside the grid.

7. CONDITIONS FOR BIMODALITY

The stationary distribution of wealth is determined by the Kolmogorov Forward Equation (Section 10), whose shape depends on the interaction between the attractor structure (Sections 4–4.3), the diffusion intensity  $\sigma$ , and the regime-switching rates  $\lambda_{LH}, \lambda_{HL}$ . In this section we identify conditions under which the ergodic distribution exhibits bimodality—two distinct modes separated by a trough—which is the distributional signature of the poverty trap.

We state the conditions as a proposition rather than a theorem, because condition (C2) involves an inequality that cannot be verified analytically in the full stochastic model and must be checked numerically for a given calibration.

**PROPOSITION 32**—Conditions for a bimodal ergodic distribution: *The stationary wealth distribution is bimodal if the following conditions hold jointly:*

- (C1) Stable interior attractors.** *The Cobb-Douglas specification with  $\alpha \in (0, 1)$  guarantees that each productivity regime  $j \in \{L, H\}$  possesses a unique, stable interior attractor  $k_j^{\text{ss}} > 0$  for any  $\rho, \delta > 0$  and  $\sigma \geq 0$  (Propositions 4 and 6). In the deterministic benchmark ( $\sigma = 0, \lambda_{LH} = \lambda_{HL} = 0$ ), the attractors admit the closed-form expression:*

$$k_j^{\text{ss}}(0) = \left( \frac{\alpha A_j}{\rho + \delta} \right)^{1/(1-\alpha)}. \quad (30)$$

*In the full stochastic model, precautionary savings, option-value effects, and regime coupling modify the attractor locations (Propositions 6 and 8), but the existence and uniqueness of a stable interior attractor per regime is preserved by the strict concavity of  $f_j$  (Proposition 23).*

- (C2) Sufficient separation between attractors.** *The two modes are distinguishable only if the distance between the coupled attractors exceeds the local dispersion induced by Brownian diffusion:*

$$k_H^{\text{ss},c} - k_L^{\text{ss},c} \gg \sigma_L^{\text{ss}} + \sigma_H^{\text{ss}}, \quad (31)$$

*where  $\sigma_j^{\text{ss}}$  is the stationary standard deviation of the wealth distribution near attractor  $j$ , which depends on  $\sigma, f_j''(k_j^{\text{ss}})$ , and the local drift structure.<sup>2</sup> In the deterministic benchmark, the separation is:*

$$k_H^{\text{ss}}(0) - k_L^{\text{ss}}(0) = \left( \frac{\alpha}{\rho + \delta} \right)^{1/(1-\alpha)} (A_H^{1/(1-\alpha)} - A_L^{1/(1-\alpha)}),$$

*which depends only on the TFP gap  $A_H/A_L$  and the structural parameters  $(\alpha, \rho, \delta)$ . In the full stochastic model, regime switching and diffusion shift both attractors (Propositions 8 and 10). The net effect on the gap is parameter-dependent: under the baseline calibration, the gap widens from 4.00 to 4.62 because the precautionary motive shifts  $k_H^{\text{ss},c}$  upward by more than it shifts  $k_L^{\text{ss},c}$ . In other regions of the parameter space—particularly when  $\lambda_{HL}$  is large, strengthening the front-loading channel for H-agents—the gap may narrow. Condition (C2) requires that, whatever the direction of the shift, the residual gap remain large relative to the diffusion-induced spread. As  $\sigma \rightarrow 0$ , the standard deviations  $\sigma_j^{\text{ss}} \rightarrow 0$  while*

---

<sup>2</sup>A local Gaussian approximation near each attractor gives  $\sigma_j^{\text{ss}} \approx \sigma / \sqrt{2|\mu'_j(k_j^{\text{ss}})|}$ , where  $\mu'_j = f'_j - \delta - c'_j$  is the derivative of the drift evaluated at the attractor. This approximation is valid when the density is sharply peaked around  $k_j^{\text{ss}}$ .

the attractor gap remains bounded away from zero, so (C2) is satisfied for sufficiently small noise.

- (C3) Interior signaling threshold.** The Skiba threshold must be interior:  $k^* \in (\phi, \infty)$ , so that signaling is feasible but not immediate (Remark 22(a)). This requires two sub-conditions:
- (a)  $\phi < k_L^{ss,c}$ : the signaling cost is below the L-attractor, so that an L-agent who receives an opportunity can, in principle, accumulate enough to signal without first needing to escape the basin.
  - (b)  $D(\phi) > 0$ : signaling is not optimal immediately upon becoming affordable. This holds when the obsolescence risk  $\lambda_{HL}$  is large enough, or the TFP gap  $A_H/A_L$  small enough, that the post-signaling wealth  $k - \phi$  is too low to justify the transition (Definition 20).

Together, (a) and (b) ensure that W-agents accumulate in the interval  $[\phi, k^*)$  before signaling—the “Frustrated Aspirants” who generate mass between the two modes. If  $k^* = \phi$  (immediate signaling), the W-state is transient and the economy behaves as a two-state model without an accumulation phase. If  $k^* = +\infty$  (no signaling), the economy collapses to a single-attractor model at  $A_L$ .

- (C4) Moderate coupling rates.** The Poisson rates  $\lambda_{LH}$  and  $\lambda_{HL}$  must be small enough that agents spend sufficient time in each regime for the local attractors to shape the distribution. Specifically:
- (a) The attractor gap  $k_H^{ss,c} - k_L^{ss,c}$  remains large relative to the diffusion-induced spread  $\sigma_L^{ss} + \sigma_H^{ss}$ . Since the coupling shifts both attractors (Propositions 8 and 10), this requires that the net effect of the shifts—whether compressive or expansive—does not reduce the gap below the threshold needed for condition (C2).
  - (b) The obsolescence rate satisfies  $\lambda_{HL} \ll 1/T_{acc}^H$ , where  $T_{acc}^H$  is the characteristic time for an H-agent to accumulate from the post-signaling entry point  $k^* - \phi$  to  $k_H^{ss,c}$ . This ensures that newly promoted H-agents have enough time to reach the upper attractor before being hit by an obsolescence shock. If  $\lambda_{HL}$  is too large, H-agents revert to L before accumulating to  $k_H^{ss,c}$ , and the right mode fails to form.
  - (c) The opportunity arrival rate satisfies  $\lambda_{LH} \ll 1/T_{acc}^W$ , where  $T_{acc}^W$  is the time for a W-agent to accumulate from  $k_L^{ss,c}$  to  $k^*$ . Combined with (b), this ensures that agents do not cycle rapidly between regimes: each agent spends enough time near her current attractor for the local restoring force to concentrate mass into a distinguishable mode. When both rates are large, agents cycle so frequently that the distribution homogenizes into a single peak.

**PROOF SKETCH:** Condition (C1) is established in Propositions 4–6. The strict concavity of  $f_j$  ensures that the drift  $\mu_j(k) = f_j(k) - c_j(k) - \delta k$  changes sign exactly once (from positive to negative) as  $k$  increases through  $k_j^{ss}$ , making  $k_j^{ss}$  a unique, stable attractor.

Condition (C2) is a separation condition on the coupled attractors. When it holds, the stationary KFE (Section 10) admits a solution with two local maxima. To see this, note that near each attractor  $k_j^{ss}$ , the drift is approximately linear:  $\mu_j(k) \approx \mu'_j(k_j^{ss})(k - k_j^{ss})$  with  $\mu'_j(k_j^{ss}) < 0$  (stability). The local density is approximately Gaussian with mean  $k_j^{ss}$  and variance  $\sigma^2/(2|\mu'_j(k_j^{ss})|)$ . When the distance between means far exceeds the sum of standard deviations, the two Gaussians have negligible overlap and the aggregate density is bimodal.

Condition (C3) ensures that the signaling mechanism is active: there exist agents in the W-state who accumulate toward  $k^*$ , creating a flow from the lower basin to the upper basin. Without this flow (i.e., when  $k^* = \infty$ ), no agent reaches the H-regime and the distribution is unimodal at  $k_L^{ss}$ .

Condition (C4) ensures that the flow between basins is slow enough for two distinct modes to emerge. Rapid cycling ( $\lambda_{LH}, \lambda_{HL}$  large) generates frequent regime changes, preventing agents from settling near either attractor and producing a broad, unimodal distribution. ■

REMARK 33—Sufficient vs. necessary conditions: Conditions (C1)–(C4) are jointly sufficient for bimodality in the following sense: when all four hold, the numerical solution of the KFE (Section 10) produces a density with two distinct local maxima. The conditions are not individually necessary—for example, bimodality can persist even when (C4c) is mildly violated, because Brownian diffusion provides an alternative (slower) channel for basin crossing. A sharp characterization of the necessary and sufficient conditions for bimodality in the full nonlinear KFE is an open problem; the conditions above identify the economically interpretable parameter restrictions under which bimodality obtains.

REMARK 34—Numerical verification: Under the baseline calibration (Table I), all four conditions are satisfied. Section 10 presents the resulting bimodal density.

## 8. NUMERICAL METHOD

The model does not admit a closed-form solution. The coupled system of HJB equations (22)–(24), together with the variational inequality for the W-state and the Kolmogorov Forward Equation for the stationary distribution, must be solved numerically. This section describes the computational strategy.

The solution proceeds in two stages that exploit a fundamental duality in the HACT framework (Achdou et al., 2022). The HJB equations govern individual optimization: given the state  $(k, s)$ , what is the optimal consumption and signaling policy? The Kolmogorov Forward Equation (KFE) governs the distributional consequences of those policies: given that all agents behave optimally, what is the stationary cross-sectional distribution of wealth? In the standard HACT literature with production economies (Achdou et al., 2022, Kaplan et al., 2018), the two stages are linked by equilibrium prices—the interest rate and the wage depend on aggregate capital, creating a fixed-point problem. In our model, the coupling is one-directional: since each agent operates her own Cobb-Douglas technology without factor market interaction, the individual problem does not depend on the wealth distribution. The HJB system can therefore be solved first, and the resulting policies fed into the KFE as given inputs.

*Stage 1: HJB system.* We discretize the capital domain  $[0, k_{\max}]$  on a uniform grid of  $N$  points and solve the coupled HJB equations using the implicit upwind finite difference scheme of Achdou et al. (2022). The upwind strategy—forward differences where the drift is positive, backward differences where it is negative—ensures monotonicity of the scheme, which is the key condition for convergence to the viscosity solution (Barles and Souganidis, 1991). The implicit time stepping guarantees unconditional stability, allowing large step sizes that accelerate convergence. Policy iteration (Howard improvement) replaces the slow contraction of value iteration with a sequence of linear solves, each of which updates the value function globally. For the W-state, we augment the standard scheme with an American projection step that enforces the constraint  $V_W(k) \geq V_H(k - \phi)$  at each iteration, following the penalty and projection methods used in computational finance for American option pricing (Wilmott et al., 1995).

*Stage 2: Kolmogorov Forward Equation.* Once the optimal policies  $\{c_j(k)\}_{j \in \{L, W, H\}}$  and the signal region  $\{k \geq k^*\}$  are determined, the stationary distribution  $\{g_L(k), g_W(k), g_H(k)\}$  is obtained from the KFE—the adjoint of the infinitesimal generator associated with the HJB operator. The KFE describes the steady-state balance of probability flows: at each point  $(k, j)$ , the

inflow of agents from drift, diffusion, and regime switching equals the outflow. The discretized KFE inherits the transpose structure of the discretized HJB (Achdou et al., 2022), ensuring consistency between the individual optimization and the distributional accounting. The non-local transfer induced by signaling—agents in  $W$  at  $k \geq k^*$  are removed and reinjected in  $H$  at  $k - \phi$ —enters the KFE as a source-sink term that connects the two basins of attraction.

The remainder of this section presents the discretization, the iterative algorithm, and the convergence diagnostics in detail.

## 9. NUMERICAL METHOD FOR THE HJB SYSTEM

### 9.1. Upwind Finite Differences

We discretize  $k \in [k_{\min}, k_{\max}]$  on a uniform grid  $\{k_1, \dots, k_N\}$  with  $k_1 = \varepsilon > 0$  (small, to avoid the singularity of  $k^{\alpha-1}$  at zero) and spacing  $\Delta k = (k_{\max} - k_{\min})/(N - 1)$ .

**DEFINITION 35**—Upwind approximation: For each grid point  $i$  and state  $j$  with production  $f_j(k_i) = A_j k_i^\alpha$ , define forward and backward approximations to the first derivative:

$$V_{j,i}^f = \frac{V_{j,i+1} - V_{j,i}}{\Delta k}, \quad V_{j,i}^b = \frac{V_{j,i} - V_{j,i-1}}{\Delta k}. \quad (32)$$

Each approximation implies a candidate consumption policy (from the first-order condition (42)) and a candidate drift:

$$c_i^f = (V_{j,i}^f)^{-1/\gamma}, \quad \mu_i^f = f_j(k_i) - c_i^f - \delta k_i, \quad (33)$$

$$c_i^b = (V_{j,i}^b)^{-1/\gamma}, \quad \mu_i^b = f_j(k_i) - c_i^b - \delta k_i. \quad (34)$$

The upwind scheme selects the approximation consistent with the direction of capital flow:

$$V'_{j,i} = \begin{cases} V_{j,i}^f & \text{if } \mu_i^f > 0 \quad (\text{accumulating: use forward difference}), \\ V_{j,i}^b & \text{if } \mu_i^b < 0 \quad (\text{decumulating: use backward difference}), \\ u'(f_j(k_i) - \delta k_i) & \text{otherwise} \quad (\text{zero drift: steady-state consumption}). \end{cases} \quad (35)$$

The third case corresponds to points where neither forward nor backward drift has the correct sign. At such points, the agent is locally at a zero-drift steady state: consumption equals net income,  $c_i = f_j(k_i) - \delta k_i$ , and the slope of the value function is  $V'_{j,i} = u'(c_i)$ .

The discretized HJB operator for state  $j$  at grid point  $i$  takes the form:

$$\rho V_{j,i} = u(c_{j,i}) + x_i V_{j,i+1} + z_i V_{j,i} + y_i V_{j,i-1} + (\text{switching terms}), \quad (36)$$

where the finite-difference coefficients encode both advection (drift) and diffusion:

$$x_i = \frac{\max(\mu_i, 0)}{\Delta k} + \frac{\sigma^2/2}{(\Delta k)^2}, \quad (37)$$

$$y_i = \frac{-\min(\mu_i, 0)}{\Delta k} + \frac{\sigma^2/2}{(\Delta k)^2}, \quad (38)$$

$$z_i = -(x_i + y_i). \quad (39)$$

The coefficient  $x_i$  governs the weight on the right neighbor  $V_{j,i+1}$  (forward advection plus diffusion),  $y_i$  governs the weight on the left neighbor  $V_{j,i-1}$  (backward advection plus diffusion), and  $z_i$  is the diagonal entry, chosen so that the row sums to zero in the generator matrix.

**PROPOSITION 36—Monotonicity and convergence:** *The upwind scheme (37)–(39) produces a system  $A_j \mathbf{V}_j = \mathbf{b}_j$  where  $A_j$  is a diagonally dominant M-matrix (positive diagonal, non-positive off-diagonal). The scheme is monotone, consistent, and converges to the unique viscosity solution of the HJB equation as  $\Delta k \rightarrow 0$ .*

**PROOF SKETCH:** By construction,  $x_i \geq 0$  and  $y_i \geq 0$  for all  $i$  (both the advection and diffusion contributions are non-negative). Since  $z_i = -(x_i + y_i) \leq 0$ , the off-diagonal entries of the generator matrix are non-positive. Incorporating the discount rate, the diagonal of  $A_j$  is  $\rho - z_i + \lambda_{\text{out},j} = \rho + x_i + y_i + \lambda_{\text{out},j} > 0$ , ensuring strict diagonal dominance. These properties make  $A_j$  an M-matrix, which guarantees that the discrete maximum principle holds: the solution is bounded by the data. Monotonicity (the scheme is non-decreasing in each  $V_{j,i'}$  for  $i' \neq i$ ) follows from the non-positivity of off-diagonal entries. Combined with consistency (the truncation error vanishes as  $\Delta k \rightarrow 0$ ) and stability (the M-matrix property provides uniform bounds), the convergence theorem of Barles and Souganidis (1991) guarantees convergence to the viscosity solution of the continuous HJB equation. ■

## 9.2. Solution Algorithm

The discretized HJB system is nonlinear: the coefficients  $x_i, y_i, z_i$  depend on the consumption policy  $c_{j,i}$ , which in turn depends on the value function  $V_{j,i}$  through the first-order condition. We solve this fixed-point problem by an implicit time-stepping scheme with Gauss–Seidel ordering across regimes and an American projection step for the variational inequality in state  $W$ .

The algorithm iterates on the three value functions in the order  $L \rightarrow W \rightarrow H$ , which follows the direction of regime transitions. At each outer iteration  $n$ :

- Step 1. Policy update.* Given the current iterate  $\mathbf{V}_j^{n-1}$ , compute the upwind approximation (35) at each grid point to obtain the consumption policy  $c_{j,i}^{n-1}$  and drift  $\mu_{j,i}^{n-1}$ . Assemble the finite-difference coefficients  $x_i, y_i, z_i$  from (37)–(39).
- Step 2. Implicit update.* For each state  $j$  in the order  $L, W, H$ , solve the tridiagonal system:

$$\left( \frac{1}{\Delta t} I + \rho I + \Lambda_j - A_j^{n-1} \right) \mathbf{V}_j^n = \frac{\mathbf{V}_j^{n-1}}{\Delta t} + \mathbf{u}_j^{n-1} + \Lambda_j \mathbf{V}_{-j}^*, \quad (40)$$

where  $\mathbf{V}_{-j}^*$  uses the *most recently updated* value functions of the other regimes (Gauss–Seidel ordering): when updating  $W$ ,  $\mathbf{V}_L^n$  is already available from the  $L$ -step; when updating  $H$ , both  $\mathbf{V}_L^n$  and  $\mathbf{V}_W^n$  are available. Each system is tridiagonal and solved in  $O(N)$  operations.

- Step 3. American projection (W-state only).* After solving for  $\mathbf{V}_W^n$ , enforce the variational inequality: for each grid point  $k_i \geq \phi$ , set

$$V_{W,i}^n \leftarrow \max(V_{W,i}^n, V_H^{n-1}(k_i - \phi)).$$

Points where the constraint binds constitute the signal region; the Skiba threshold  $k^*$  is the lowest such point. The consumption policy and drift in the signal region are then recomputed from the projected value function to ensure consistency with the KFE.

- Step 4. Convergence check.* Stop if  $\max_j \|\mathbf{V}_j^n - \mathbf{V}_j^{n-1}\|_\infty < \varepsilon_{\text{tol}}$ .

The implicit scheme is unconditionally stable, allowing arbitrarily large time steps. Following Achdou et al. (2022), we increase  $\Delta t$  geometrically as the iteration converges: in the limit  $\Delta t \rightarrow \infty$ , each implicit step becomes an exact policy evaluation, and the algorithm reduces to Howard’s policy iteration. Under the baseline calibration, convergence to  $\varepsilon_{\text{tol}} = 10^{-8}$  is achieved in 8 iterations. Appendix 15.4 provides the full algorithmic details and convergence analysis.

## 10. KOLMOGOROV FORWARD EQUATION

The stationary wealth distribution is the solution to the Kolmogorov Forward Equation (KFE)—the adjoint of the HJB operator—subject to the non-local transfer induced by signaling. For the sake of brevity, Appendix 15.5 derives the discretized KFE system, describes the signaling transfer mechanism, and characterizes the properties of the resulting ergodic distribution.

## 11. CALIBRATION AND NUMERICAL EXPERIMENT

The purpose of this section is not to match a specific economy but to demonstrate that the model generates a bimodal stationary distribution—the Twin Peaks—under empirically plausible parameter values. We adopt a baseline calibration that places the economy in the interior-threshold regime (Remark 22(a)), where signaling is feasible but not immediate, producing a non-trivial wait zone and the full range of agent types described in the introduction. Table I reports the baseline parameters. We group them into four categories: preferences, technology, stochastic environment, and signaling. For each parameter, we adopt standard values from the literature where available and discuss our choices in detail in Appendix 15.6.

The next section presents the results of this experiment: the value functions, optimal policies, signaling surplus, and the stationary distribution.

## 12. RESULTS

This section presents the numerical results under the baseline calibration of Table I. We first build intuition for the equilibrium structure, then verify the theoretical predictions and examine the consumption diagnostics that constitute the paper’s central empirical prediction.

### 12.1. Results in a Nutshell

Before examining the numerical output in detail, it is useful to build intuition for the equilibrium structure through three complementary perspectives: the spatial organization of the state space, the value functions that govern individual decisions, and the resulting stationary densities. Figures 1–3 present these perspectives under the baseline calibration.

*The geography of the trap.* Figure 1 displays the partition of the capital axis induced by the signaling friction. The economy is divided into three regions whose boundaries are determined by two structural parameters—the signaling cost  $\phi$  and the endogenous Skiba threshold  $k^*$ —and whose economic logic is fundamentally different.

Below  $\phi = 9$ , agents are too poor to afford the credential: even if a signaling opportunity arises ( $\lambda_{LH}$ ), they cannot exercise it. This is the region of *absolute* exclusion, where the poverty trap operates through a wealth constraint that is, in a precise sense, analogous to a borrowing constraint in the Bewley tradition—except that here the constraint binds on the *investment* margin rather than on consumption. Between  $\phi$  and  $k^* = 13.4$  lies the *wait zone*: agents can

TABLE I  
BASELINE CALIBRATION

Parameter	Description	Value	Reference / Target
<i>Preferences</i>			
$\gamma$	Risk aversion (CRRA)	2.0	Standard; Lucas (1987), Attanasio (1999), Chetty (2006)
$\rho$	Discount rate	0.05	Annual; Achdou et al. (2022)
<i>Technology</i>			
$\alpha$	Capital elasticity	0.33	Standard in Cobb-Douglas calibrations
$\delta$	Depreciation rate	0.02	Low; broad capital interpretation
$A_L$	Low-regime TFP	1.0	Normalization
$A_H$	High-regime TFP	1.25	Conservative; college premium $\approx 60\text{--}80\%$ (Goldin and Katz (2008))
<i>Stochastic environment</i>			
$\sigma$	Diffusion coefficient	0.30	Calibrated to match wealth dispersion
$\lambda_{LH}$	Opportunity arrival rate	0.005	Schumpeterian long waves; Comin and Hobijn (2010)
$\lambda_{HL}$	Obsolescence rate	0.002	Persistent regimes; Azariadis and Stachurski (2005)
<i>Signaling</i>			
$\phi$	Signaling cost	9.0	Interior Skiba; $\phi < k_L^{\text{ss},c} < k^*$
<i>Computational</i>			
$N$	Grid points	501	
$k_{\max}$	Upper grid boundary	50	
$\Delta t$	Implicit time step	500	
$\epsilon_{\text{tol}}$	Convergence tolerance	$10^{-8}$	
$\bar{\lambda}$	Signaling drain rate (KFE)	$10^3$	

afford the cost but *choose* not to pay it, because the post-signaling wealth  $k - \phi$  would leave them too far below the H-attractor, exposed to obsolescence risk with insufficient buffer. This is the region of *rational* exclusion—the novel mechanism of our model. Above  $k^*$ , agents signal immediately upon opportunity arrival.

The critical observation is the position of the L-attractor:  $k_L^{\text{ss},c} = 11.5$  falls *inside* the wait zone ( $\phi < k_L^{\text{ss},c} < k^*$ ). This means that the typical low-productivity agent is neither too poor to signal nor unwilling to signal in principle—she is stuck in a region where signaling is affordable but not yet optimal. The trap is not a corner solution but an interior one, and this is what makes it invisible to standard diagnostic tests.

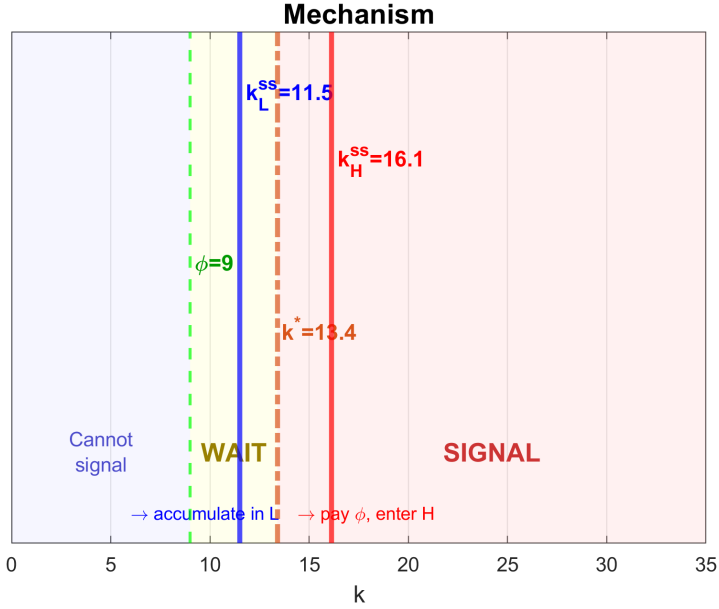


FIGURE 1.—Partition of the capital axis under the baseline calibration. The signaling cost  $\phi = 9$  and the endogenous Skiba threshold  $k^* = 13.4$  divide the state space into three regions: absolute exclusion ( $k < \phi$ ), the wait zone ( $\phi \leq k < k^*$ , shaded in yellow), and immediate signaling ( $k \geq k^*$ ). The coupled attractors  $k_L^{ss,c} = 11.5$  and  $k_H^{ss,c} = 16.1$  are shown as solid vertical lines. The L-attractor lies inside the wait zone: the typical trapped agent *can* afford to signal but *chooses* not to.

*Why the trap is self-enforcing.* Figure 2 reveals the economic forces behind the partition. The three value functions  $V_L$ ,  $V_W$ ,  $V_H$  are strictly concave (Proposition 23) and strictly ordered:  $V_H(k) > V_W(k) > V_L(k)$  for all  $k > 0$  (Proposition 24). The ordering reflects the value of options:  $V_H$  incorporates the benefit of high productivity,  $V_W$  adds the option to signal, and  $V_L$  has neither.

The signaling decision is governed by the comparison between  $V_W(k)$ —the value of holding the option—and  $V_H(k - \phi)$ —the value of exercising it. The dotted curve  $V_H(k - \phi)$  is simply  $V_H$  shifted rightward by  $\phi$ : paying the signaling cost is equivalent to starting the H-regime with  $\phi$  fewer units of capital. At low wealth, this shift is devastating—the concavity of  $V_H$  means that the marginal value of the lost capital is very high, so  $V_W(k) \gg V_H(k - \phi)$  and the agent waits. As wealth increases, the gap narrows because the marginal cost of losing  $\phi$  units falls (the function flattens). At  $k = k^*$ , the two curves cross:  $V_W(k^*) = V_H(k^* - \phi)$ , and the agent is indifferent—this is the Skiba threshold.

The mechanism is self-enforcing because of the drift structure. At  $k_L^{ss,c}$ , the drift  $\mu_L$  is zero: the agent has no incentive to accumulate further under  $A_L$  technology, so she *cannot* drift into the signal region through savings alone. Only the exogenous arrival of an opportunity ( $\lambda_{LH}$ ) moves her to the W-state, and even then, she must accumulate from  $k_L^{ss,c} = 11.5$  to  $k^* = 13.4$ —an additional 1.9 units of capital—before signaling becomes optimal. During this accumulation phase, she is vulnerable to losing the opportunity before reaching  $k^*$ .

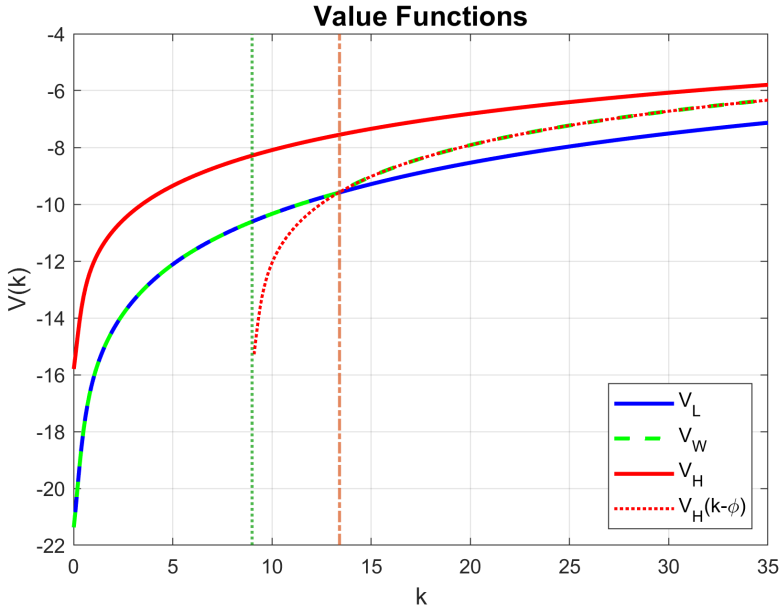


FIGURE 2.—Value functions under the baseline calibration.  $V_H > V_W > V_L$  for all  $k > 0$  (Proposition 24). All three are strictly concave (Proposition 23). The shifted function  $V_H(k - \phi)$  (dotted) crosses  $V_W$  at the Skiba threshold  $k^* = 13.4$ : below this point, the concavity of  $V_H$  makes the capital loss from paying  $\phi$  too costly; above it, the agent signals immediately. The green dotted line marks  $\phi = 9$ , below which signaling is infeasible.

*The resulting polarization.* Figure 3 displays the stationary densities decomposed by productivity regime—the observable counterpart of the theoretical structure. The bimodal shape predicted by Proposition 32 is immediately apparent, but the decomposition reveals *why* the two peaks arise and why they persist.

The left mode, centered near  $k_L^{ss,c}$ , is dominated by the L-density  $g_L$  (blue). These are agents who have never received an opportunity, or who received one and lost it before reaching  $k^*$ . The concentration of mass near the attractor reflects the restoring force of the drift: agents who are perturbed away from  $k_L^{ss,c}$  by the diffusion  $\sigma$  are pulled back by the negative drift above  $k_L^{ss,c}$  and positive drift below it. The right mode, centered near  $k_H^{ss,c}$ , is dominated by the H-density  $g_H$  (red). These are agents who have successfully signaled and are enjoying the returns to high productivity. The peak is sharper and taller, reflecting the stronger restoring force at  $k_H^{ss,c}$  (where the curvature of  $f_H$  is larger due to higher TFP).

The W-density  $g_W$  (green dashed) is small but structurally revealing. It is concentrated in the interval  $[\phi, k^*]$ —precisely the wait zone of Figure 1—and vanishes above  $k^*$ , where agents signal immediately. Its mass ( $\pi_W = 11.8\%$ ) represents the population of Frustrated Aspirants: agents who hold a signaling opportunity but have not yet accumulated enough to exercise it. The existence of this intermediate group—neither trapped nor free—is a distinctive prediction of the model, absent from both the Bewley tradition (which lacks regime switching) and the Galor-Zeira tradition (which lacks the option-value margin).

A striking feature of the figure is that the three densities overlap extensively. This overlap is not noise—it is generated by the flows between regimes and constitutes one of the model’s sharpest empirical implications: capital alone does not identify an agent’s state; two households with identical wealth can be on opposite trajectories. Three overlap zones are visible, each with a distinct economic story.

In the region  $k \in [4, \phi]$ , the left tail of  $g_H$  runs beneath  $g_L$ . The H-agents here are *newly signaled*: they entered state H at  $k^* - \phi = 4.4$  and are accumulating rapidly toward  $k_H^{ss,c}$ . The density is thin because the drift  $\mu_H$  is strongly positive at low capital—agents transit through this zone quickly, like a fast current through a narrow channel. Their L-counterparts at the same capital level are in a fundamentally different situation: slowly accumulating toward  $k_L^{ss,c}$  under low productivity  $A_L$ , with much lower savings rates. An econometrician observing two households with  $k = 6$  would find radically different consumption behavior—the H-agent saving aggressively (high marginal return  $f'_H(6)$ ), the L-agent consuming most of her income—yet no cross-sectional variable other than the productivity regime would distinguish them.

In the wait zone  $k \in [\phi, k^*]$ , all three densities coexist. This is the most economically complex region of the state space:  $g_L$  is approaching its peak (we are near  $k_L^{ss,c} = 11.5$ );  $g_W$  has its entire support here, representing Frustrated Aspirants who hold the signaling option and are saving toward  $k^*$ ; and  $g_H$  is still present as a transit flow of recently promoted agents climbing toward  $k_H^{ss,c}$ . Three agents with  $k = 11$  can be in entirely different situations: one trapped without an opportunity (L), one racing to accumulate the last 2.4 units before the opportunity expires (W), and one freshly credentialed and building her buffer (H). Their MPCs differ, their APCs differ, and their future trajectories diverge completely—yet in a household survey they are observationally identical without information on the productivity regime.

In the region  $k \in [k^*, 20]$ , the right tail of  $g_L$  runs beneath the peak of  $g_H$ . The L-agents here are the *Decaying Rentiers*—former H-agents who suffered the obsolescence shock ( $\lambda_{HL}$ ) and reverted to low productivity. The shock changes the regime instantaneously but does not destroy capital: these agents retain high wealth but now face a negative drift under  $A_L$  technology, which cannot sustain such a capital stock. They are decumulating toward  $k_L^{ss,c}$ , consuming more than their net income. They are the mirror image of the newly signaled agents in the left tail of  $g_H$ : same wealth region, opposite direction, opposite regime. The symmetry between these two transit populations—one ascending in H, one descending in L—is a direct consequence of the Poisson switching structure and illustrates why regime identification is essential for any empirical test of the model.

The valley between the two peaks—the region around  $k^*$ —has near-zero density. This is not an accident: agents in the W-state who reach  $k^*$  signal immediately, removing themselves from the W-density and re-entering as H-agents at  $k^* - \phi$ . The signaling threshold acts as an absorbing barrier for the wait state, creating a structural gap in the distribution that separates the two clubs. The depth of this valley—rather than the distance between the peaks—is the most robust measure of the strength of the poverty trap.

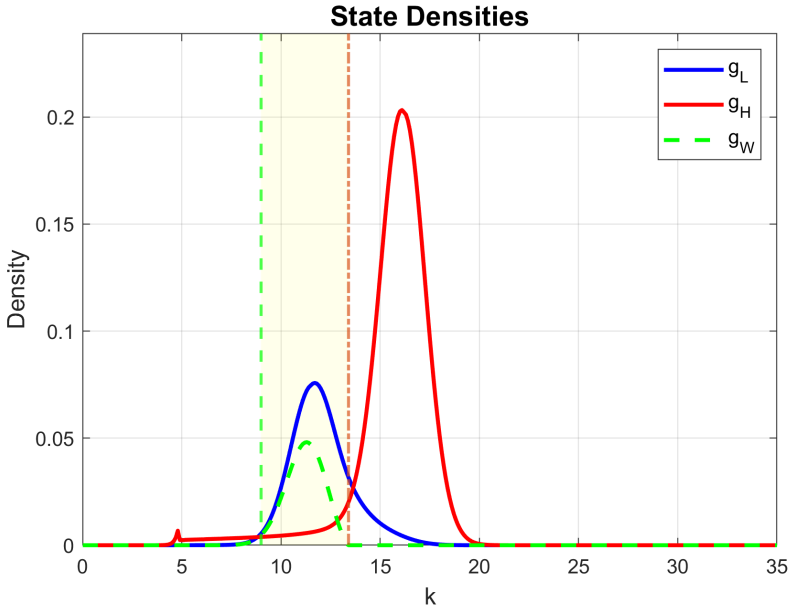


FIGURE 3.—Stationary densities by regime. The L-density  $g_L$  (blue) peaks near  $k_L^{ss,c} = 11.5$ , forming the poverty trap mode; the H-density  $g_H$  (red) peaks near  $k_H^{ss,c} = 16.1$ , forming the accumulation mode. The W-density  $g_W$  (green dashed) is confined to the wait zone  $[\phi, k^*]$  and vanishes above  $k^*$ , where signaling is immediate. The three densities overlap extensively: in  $[4, \phi]$ , newly signaled H-agents transit rapidly alongside slowly accumulating L-agents; in  $[\phi, k^*]$ , all three populations coexist; in  $[k^*, 20]$ , Decaying Rentiers (L) slide back through the region dominated by H-agents. The valley near  $k^*$  reflects the absorbing-barrier effect: agents who reach the threshold exit the W-state and re-enter as H-agents at  $k^* - \phi$ . Ergodic shares:  $\pi_L = 25.2\%$ ,  $\pi_W = 11.8\%$ ,  $\pi_H = 63.0\%$ .

### 12.2. Numerical Verification

We now verify that the simulation output is consistent with the theoretical predictions of Sections 3–7.

*Convergence.* The HJB solver (Algorithm 1) converges in 8 iterations to a tolerance of  $10^{-8}$ . The coupled attractors are  $k_L^{ss,c} = 11.50$  and  $k_H^{ss,c} = 16.12$ , both above their deterministic counterparts ( $k_L^{ss}(0) = 10.12$ ,  $k_H^{ss}(0) = 14.12$ ). The L-attractor rises by 13.6%, driven by the precautionary motive and the option value of signaling opportunities (Propositions 6 and 8). The H-attractor rises by 14.2%, confirming that the precautionary channel dominates the front-loading effect (Proposition 10). The attractor gap widens modestly from 4.00 to 4.62.

*Skiba threshold.* The threshold is  $k^* = 13.40$ , producing an interior signaling regime (Remark 22(a)) with a wait zone of width  $k^* - \phi = 4.40$ . The signaling surplus  $D(k)$  declines monotonically from  $D(\phi) = 5.25$  to  $D(k^*) = 0$ , and the L-attractor lies inside the wait zone ( $\phi < k_L^{ss,c} < k^*$ ), confirming the structural trap mechanism.

*Bimodality.* The stationary distribution is bimodal, with ergodic shares  $\pi_L = 25.2\%$ ,  $\pi_W = 11.8\%$ ,  $\pi_H = 63.0\%$ . Mean wealth is  $\mathbb{E}[k] = 14.23$  and the Gini coefficient is 0.104. The modest Gini reflects the conservative TFP gap ( $A_H/A_L = 1.25$ ); the relevant diagnostic of the poverty trap is the bimodality of the distribution, not the level of inequality.

*Euler equation.* At both attractors, the drift is numerically zero ( $|\mu_j(k_j^{ss,c})| < 10^{-6}$ ), confirming the zero-drift condition. The net marginal return  $f'_j(k_j^{ss,c}) - \delta = 0.044$  falls below  $\rho = 0.050$

by 0.006, representing the combined precautionary and switching corrections in the Euler equation (48). The near-equality of net returns across regimes ( $f'_L - \delta \approx f'_H - \delta \approx 0.044$ ) reflects the symmetric structure of the zero-drift condition: at both attractors, the risk-adjusted return, net of all corrections, equals  $\rho$ .

### 12.3. The MPC/APC Diagnostic

The central empirical prediction concerns the joint behavior of the marginal propensity to consume out of wealth ( $\partial c/\partial k$ ) and the average propensity to consume ( $c/Y$ ). Table II reports these statistics at the two attractors.

TABLE II  
MPC AND APC AT THE ATTRACTORS

	$\partial c_j/\partial k$	$c_j/Y_j$	$f'_j - \delta$	Drift $\mu_j$
L-attractor ( $k = 11.50$ )	0.055	0.897	0.044	$\approx 0$
H-attractor ( $k = 16.12$ )	0.073	0.897	0.044	$\approx 0$
Benchmark $\rho$	0.050	—	0.050	—

At  $k_L^{ss,c}$ , the MPC is  $0.055 \approx \rho$ : a windfall  $\Delta k$  raises consumption by only  $\rho \cdot \Delta k$  per unit time. The agent has no incentive to save the transfer—the net marginal return is approximately  $\rho$ , just enough to compensate impatience—so it is absorbed into consumption while capital remains practically unchanged at  $k_L^{ss,c}$ . Meanwhile, her APC is 0.897: she consumes nearly all her income, saving nothing in net terms.

This combination—low MPC, high APC—is the diagnostic signature of the structural trap. Under the standard Bewley-Kaplan-Violante framework, low MPC signals financial comfort and high APC signals financial stress. In our model, both are consequences of the zero-drift condition at a low-productivity attractor. The agent is not “hitting a wall” (a binding constraint, which would produce *high* MPC) but “sitting in a hole” (a low-productivity basin, which produces low MPC and high APC simultaneously).

The population-weighted MPCs confirm the cross-sectional pattern:

$$\begin{aligned} \mathbb{E}[\partial c/\partial k \mid L] &= 0.090, & \mathbb{E}[\partial c/\partial k \mid W] &= 0.085, \\ \mathbb{E}[\partial c/\partial k \mid H] &= 0.097, & \mathbb{E}[\partial c/\partial k] &= 0.094. \end{aligned}$$

The L/H ratio is 0.93: structurally trapped agents have *lower* marginal responsiveness to wealth than high-productivity agents, despite being poorer. This is the opposite of what a borrowing constraint model predicts and provides a testable cross-sectional implication.

### 12.4. Agent Phenotypes

The simulation identifies five distinct phenotypes, characterized by their position in the state-capital space and their consumption diagnostics:

- (i) *Hand-to-mouth* ( $k < 2$ , state L): negligible share ( $< 0.01\%$ ). High MPC ( $\approx 0.25$ ), low APC ( $\approx 0.64$ ). The closest analogue to the Bewley-Kaplan-Violante constrained agent.
- (ii) *Structurally trapped* ( $\phi < k \approx k_L^{ss,c}$ , state L): share  $\approx 20\%$ . Low MPC ( $\approx \rho$ ), high APC ( $\approx 0.90$ ). At the zero-drift interior optimum.
- (iii) *Frustrated Aspirants* (state W, wait zone): share 11.8%. MPC slightly below the L-average because the option value raises the shadow price of wealth.

- (iv) *Decaying Rentiers* ( $k > k^*$ , state L): share 4.2%. Former H-agents sliding back toward  $k_L^{ss,c}$  after the obsolescence shock. Low MPC, temporarily high capital.
- (v) *Successful signalers* (state H): share 63.0%. MPC  $\approx 0.097$ , concentrated near  $k_H^{ss,c}$ .

### 13. POLICY IMPLICATIONS

The model’s central implication for policy is that the standard toolkit—wealth transfers and credit relaxation—is ineffective against structural traps. An agent at  $k_L^{ss,c}$  who receives a transfer  $\Delta k$  has no incentive to save it: the net marginal return is approximately  $\rho$ , so the windfall is absorbed into consumption and capital drifts back to  $k_L^{ss,c}$ . The transfer is palliative, not structural. Effective policy must instead alter the parameters that define the trap: the signaling cost, the opportunity arrival rate, or the obsolescence rate.

#### 13.1. Policy Channels

The model identifies four distinct channels, each targeting a different source of immobility.

*Reducing the signaling cost  $\phi$ .* This is the most powerful lever. A lower  $\phi$  simultaneously makes signaling affordable at lower wealth and lowers the Skiba threshold  $k^*$ , shrinking the wait zone and increasing the flow from L to H. In the limit  $\phi \rightarrow 0$ , signaling is immediate upon opportunity arrival and the poverty trap vanishes. Concrete examples include tuition subsidies, credential recognition programs, and reduced barriers to professional licensing. The comparative statics confirm that as  $\phi$  increases, the economy transitions through the three regimes of Remark 22: immediate signaling, interior threshold (the baseline), and no signaling ( $k^* = \infty$ , H-density identically zero).

*Increasing opportunity arrival  $\lambda_{LH}$ .* A higher  $\lambda_{LH}$  raises the option value for L-agents, pushing  $k_L^{ss,c}$  upward (Proposition 8) and increasing the flow into the H-regime. This is the channel through which labor market institutions operate: job matching services, information networks, and credential transparency all increase the rate at which low-productivity agents encounter signaling opportunities. However, very high  $\lambda_{LH}$  accelerates turnover between regimes, potentially merging the two modes into a single peak (condition C3 of Section 7).

*Reducing obsolescence risk  $\lambda_{HL}$ .* A lower  $\lambda_{HL}$  yields a double dividend: it extends the expected duration of the H-regime, making signaling more attractive (lowering  $k^*$ ), and it extends the window for W-agents to accumulate toward  $k^*$  before losing the opportunity. Policies targeting continuous professional development, retraining, and adaptive credentialing operate through this channel.

*Raising the TFP gap  $A_H/A_L$ .* A larger productivity gap widens the distance between attractors and raises the return to signaling, lowering  $k^*$ . Both effects increase  $\pi_H$ , but also deepen polarization: the average agent is richer, while the trapped agents are relatively worse off. In practice, this corresponds to investments in the *quality* of human capital (raising the productivity premium of education) rather than its accessibility.

#### 13.2. Comparative Statics

We briefly discuss how the remaining structural parameters affect the equilibrium, focusing on the three objects that define the trap:  $k^*$ , the attractor gap  $k_H^{ss,c} - k_L^{ss,c}$ , and the ergodic shares.

*Capital elasticity*  $\alpha$ . As  $\alpha$  increases toward 1, diminishing returns weaken: the attractors move rightward and farther apart, but the basins become shallower, allowing the diffusion to spread each mode. In the limit  $\alpha \rightarrow 1$ , stable interior attractors vanish (Remark 1) and the poverty trap disappears. A lower  $\alpha$  strengthens the trap by sharpening diminishing returns and steepening the basins.

*Diffusion*  $\sigma$ . Larger  $\sigma$  spreads each mode (the stationary standard deviation scales as  $\sigma/\sqrt{2|\mu'_j(k_j^{ss,c})|}$ ) and strengthens the precautionary motive, shifting both attractors upward (Proposition 6). For bimodality, the attractor gap must exceed the combined spread (condition C2): sufficiently large  $\sigma$  merges the two modes into one.

### 13.3. Diagnostic Implications

The MPC/APC taxonomy provides a practical tool for identifying the nature of deprivation and directing interventions accordingly. Table III summarizes the mapping from observables to policy.

TABLE III  
DIAGNOSTIC GUIDE: FROM OBSERVABLES TO POLICY

Phenotype	MPC	APC	Drift	Intervention
Liquidity constrained	High	Low	$\mu > 0$	Wealth transfer
Structurally trapped	Low	High	$\mu = 0$	Reduce $\phi$ or raise $\lambda_{LH}$
Frustrated Aspirant	Low	High	$\mu > 0$	Reduce $k^*$ or slow $\lambda_{HL}$
Decaying Rentier	Low	High	$\mu < 0$	Slow $\lambda_{HL}$

Standard consumption-based tests detect only the first group (high MPC). The structurally trapped, Frustrated Aspirants, and Decaying Rentiers—who together account for over 35% of the population—are invisible to these tests because their low MPC mimics the signature of an unconstrained optimizer. An empirical strategy that conditions on *both* MPC and APC can separate the two populations and target interventions accordingly: transfers to the liquidity constrained, structural reforms for the trapped.

## 14. CONCLUSION

This paper embeds a signaling friction into the continuous-time heterogeneous agent framework. Agents operate Cobb-Douglas technologies with regime-specific productivity  $A_j \in \{A_L, A_H\}$  and face stochastic arrival of signaling opportunities and skill obsolescence risk. The optimal stopping problem—when to pay the lump-sum cost  $\phi$  to upgrade productivity—generates an endogenous Skiba threshold  $k^*$  that partitions the state space into three regions: absolute exclusion, rational exclusion (the wait zone), and immediate signaling. The stationary distribution exhibits Twin Peaks, with agents in three distinct states coexisting at the same wealth levels.

The paper's main contribution is to identify a structurally distinct form of poverty trap and its diagnostic signature. The trap is an interior optimum, not a corner solution: at the L-attractor, diminishing returns have driven the risk-adjusted marginal return to saving down to the discount rate, so no further accumulation is optimal. The agent is not constrained—she is rationally immobile. This produces a consumption signature that is invisible to standard tests: low MPC out of wealth ( $\partial c/\partial k \approx \rho$ ) combined with high APC ( $c/Y \approx 0.90$ ). The MPC alone would

classify the agent as unconstrained; the APC alone would suggest financial stress. Only the joint observation reveals the trap.

A second contribution is to show that capital alone is insufficient to identify an agent's position in the polarization dynamics. The decomposition of the stationary distribution by regime reveals that structurally trapped, waiting, and successfully upgraded agents coexist at the same wealth levels with radically different consumption behavior and mobility prospects. This has direct implications for empirical work: any test of the model requires information on the productivity regime, not only on wealth.

The model also delivers a behavioral taxonomy that maps naturally onto policy. The MPC/APC diagnostic separates agents who need transfers (liquidity constrained, high MPC) from those who need structural reform (trapped, low MPC). The most effective intervention targets the signaling cost  $\phi$ —through subsidized training, credential reform, or lower barriers to entry—rather than the wealth level. Slowing obsolescence ( $\lambda_{HL}$ ) yields a double dividend by simultaneously raising the value of the H-regime and extending the window for reaching  $k^*$ .

Several extensions are natural. First, decomposing  $\lambda_{HL}$  into separate rates for opportunity loss ( $W \rightarrow L$ ) and obsolescence ( $H \rightarrow L$ ) would break the common-rate symmetry and allow for richer policy analysis. Second, embedding the model in an overlapping generations framework would connect the signaling decision to intergenerational mobility (Chetty et al., 2014). Third, introducing endogenous wages through a matching model would allow for general equilibrium effects on the productivity premium. Finally, the consumption diagnostic is testable with household panel data: the model predicts a cluster of households with simultaneously low MPC and high APC that standard tests would classify as unconstrained but that are, in fact, structurally immobile.

## REFERENCES

- ACHDOU, YVES, JIEQUN HAN, JEAN-MICHEL LASRY, PIERRE-LOUIS LIONS, AND BENJAMIN MOLL (2022): "Income and Wealth Distribution in Macroeconomics: A Continuous-Time Approach," *The Review of Economic Studies*, 89 (1), 45–86.
- AHN, SEHYOUN, GREG KAPLAN, BENJAMIN MOLL, THOMAS WINBERRY, AND CHRISTIAN WOLF (2018): "When inequality matters for macro and macro matters for inequality," *NBER Macroeconomics Annual*, 32 (1), 1–75.
- AIYAGARI, S RAO (1994): "Uninsured idiosyncratic risk and aggregate saving," *The Quarterly Journal of Economics*, 109 (3), 659–684.
- ANGELETOS, GEORGE-MARIOS, DAVID LAIBSON, ANDREA REPETTO, JEREMY TOBACMAN, AND STEPHEN WEINBERG (2001): "The Hyperbolic Consumption Model: Calibration, Simulation, and Empirical Evaluation," *Journal of Economic Perspectives*, 15 (3), 47–68.
- ATTANASIO, ORAZIO P. (1999): "Consumption," in *Handbook of Macroeconomics*, ed. by John B. Taylor and Michael Woodford, Amsterdam: Elsevier, vol. 1B, chap. 11, 741–812.
- AUCLERT, ADRIEN (2019): "Monetary Policy and the Redistribution Channel," *American Economic Review*, 109 (6), 2333–2367.
- AUTOR, DAVID H, FRANK LEVY, AND RICHARD J MURNANE (2003): "The skill content of recent technological change: An empirical exploration," *The Quarterly Journal of Economics*, 118 (4), 1279–1333.
- AZARIADIS, COSTAS AND ALLAN DRAZEN (1990): "Threshold externalities in economic development," *The Quarterly Journal of Economics*, 105 (2), 501–526.
- AZARIADIS, COSTAS AND JOHN STACHURSKI (2005): "Poverty Traps," *Handbook of Economic Growth*, 1, 295–384.
- BANERJEE, ABHIJIT V AND ANDREW F NEWMAN (1993): "Occupational choice and the process of development," *Journal of Political Economy*, 101 (2), 274–298.
- BARLES, GUY AND PANAGIOTIS E SOUGANIDIS (1991): "Convergence of approximation schemes for fully nonlinear second order equations," *Asymptotic Analysis*, 4 (3), 271–283.
- BEWLEY, TRUMAN (1986): "Stationary monetary equilibrium with a continuum of independently fluctuating consumers," in *Contributions to Mathematical Economics in Honor of Gérard Debreu*, North-Holland, 79–102.

- BRYNJOLFSSON, ERIK AND ANDREW MCAFEE (2014): *The second machine age: Work, progress, and prosperity in a time of brilliant technologies*, WW Norton & Company.
- BUERA, FRANCISCO J, JOSEPH P KABOSKI, AND YONGSEOK SHIN (2011): “Finance and development: A tale of two sectors,” *American Economic Review*, 101 (5), 1964–2002.
- CARROLL, CHRISTOPHER D. (2001): “A Theory of the Consumption Function, with and without Liquidity Constraints,” *Journal of Economic Perspectives*, 15 (3), 23–45.
- CHETTY, RAJ (2006): “A New Method of Estimating Risk Aversion,” *American Economic Review*, 96 (5), 1821–1834.
- CHETTY, RAJ, NATHANIEL HENDREN, PATRICK KLINE, AND EMMANUEL SAEZ (2014): “Where Is the Land of Opportunity? The Geography of Intergenerational Mobility in the United States,” *The Quarterly Journal of Economics*, 129 (4), 1553–1623.
- COMIN, DIEGO AND BART HOBIJN (2010): “An Exploration of Technology Diffusion,” *American Economic Review*, 100 (5), 2031–2059.
- CRANDALL, MICHAEL G AND PIERRE-LOUIS LIONS (1983): “Viscosity solutions of Hamilton-Jacobi equations,” *Transactions of the American Mathematical Society*, 277 (1), 1–42.
- FLEMING, WENDELL H AND HALIL METE SONER (2006): *Controlled Markov Processes and Viscosity Solutions*, Springer Science & Business Media, 2nd ed.
- GALOR, ODED AND JOSEPH ZEIRA (1993): “Income distribution and macroeconomics,” *The Review of Economic Studies*, 60 (1), 35–52.
- GIANNINI, MASSIMO (2003): “Accumulation and distribution of human capital: the interaction between individual and aggregate variables,” *Economic Modelling*, 20 (6), 1053–1081.
- GOLDIN, CLAUDIA AND LAWRENCE F KATZ (2008): *The race between education and technology*, Harvard University Press.
- GOOS, MAARTEN AND ALAN MANNING (2007): “Lousy and lovely jobs: The rising polarization of work in Britain,” *The Review of Economics and Statistics*, 89 (1), 118–133.
- HSIEH, CHANG-TAI AND PETER J. KLENOW (2009): “Misallocation and Manufacturing TFP in China and India,” *The Quarterly Journal of Economics*, 124 (4), 1403–1448.
- KAPLAN, GREG, BENJAMIN MOLL, AND GIOVANNI L VIOLANTE (2018): “Monetary policy according to HANK,” *American Economic Review*, 108 (3), 697–743.
- KAPLAN, GREG AND GIOVANNI L. VIOLANTE (2014): “A Model of the Consumption Response to Fiscal Stimulus Payments,” *Econometrica*, 82 (4), 1199–1239.
- LA PORTA, RAFAEL AND ANDREI SHLEIFER (2014): “Informality and Development,” *Journal of Economic Perspectives*, 28 (3), 109–126.
- LAIBSON, DAVID (1997): “Golden Eggs and Hyperbolic Discounting,” *Quarterly Journal of Economics*, 112 (2), 443–478.
- LUCAS, JR., ROBERT E. (1987): *Models of Business Cycles*, Oxford: Basil Blackwell.
- MOLL, BENJAMIN (2014): “Productivity losses from financial frictions: Can self-financing undo capital misallocation?” *American Economic Review*, 104 (10), 3186–3221.
- OECD (2019): *Under Pressure: The Squeezed Middle Class*, OECD Publishing.
- QUAH, DANNY T (1996): “Twin peaks: growth and convergence in models of distribution dynamics,” *The Economic Journal*, 106 (437), 1045–1055.
- (1997): “Empirics for economic growth and convergence,” *European Economic Review*, 41 (3-5), 913–922.
- RESTUCCIA, DIEGO AND RICHARD ROGERSON (2008): “Policy Distortions and Aggregate Productivity with Heterogeneous Establishments,” *Review of Economic Dynamics*, 11 (4), 707–720.
- WILMOTT, PAUL, JEFF DEWYNNE, AND SAM HOWISON (1995): *The Mathematics of Financial Derivatives*, Cambridge University Press.

## 15. APPENDIX

### 15.1. Proof of Proposition 23

PROOF: We prove the result for  $V_L$ ; the argument for  $V_H$  is identical, and the result for  $V_W$  follows by an additional argument addressing the signaling option.

*Step 1: Concavity of  $V_L$  and  $V_H$ .* Fix a regime  $j \in \{L, H\}$  and consider two initial conditions  $k^a, k^b \in (0, \infty)$  with  $k^a \neq k^b$ . Let  $\{c_t^a\}$  and  $\{c_t^b\}$  denote the respective optimal consumption policies, and let  $\{k_t^a\}$  and  $\{k_t^b\}$  denote the resulting capital paths. For  $\theta \in (0, 1)$ , define  $k_0^\theta =$

$\theta k_0^a + (1 - \theta)k_0^b$  and consider the *feasible* (not necessarily optimal) policy  $c_t^\theta = \theta c_t^a + (1 - \theta)c_t^b$  starting from  $k_0^\theta$ .

Since the state equation (13) is linear in  $(k, c)$  for a given Brownian path  $\{W_t\}$  (the drift  $f_j(k) - c - \delta k$  is concave in  $k$  and linear in  $c$ , and the diffusion  $\sigma$  is constant), the capital path under  $c_t^\theta$  satisfies, pathwise:

$$k_t^\theta \geq \theta k_t^a + (1 - \theta)k_t^b \quad \text{for all } t \geq 0,$$

where the inequality follows from the concavity of  $f_j(k) = A_j k^\alpha$  in  $k$  ( $\alpha < 1$ ). By strict concavity of the CRRA utility function  $u$ :

$$u(c_t^\theta) = u(\theta c_t^a + (1 - \theta)c_t^b) > \theta u(c_t^a) + (1 - \theta)u(c_t^b).$$

Taking expectations and integrating:

$$V_j(k_0^\theta) \geq \mathbb{E} \left[ \int_0^\infty e^{-\rho t} u(c_t^\theta) dt \right] > \theta V_j(k_0^a) + (1 - \theta) V_j(k_0^b),$$

where the first inequality uses the fact that  $c_t^\theta$  is feasible (but not necessarily optimal) from  $k_0^\theta$ , and the second uses the strict concavity of  $u$ . This establishes strict concavity of  $V_j$  on  $(0, \infty)$ .

*Step 2: Extension to  $V_W$ .* The W-agent has the same production function as the L-agent ( $A_L k^\alpha$ ) plus an additional option: the right to signal at a self-chosen time  $\tau$ . The argument of Step 1 applies to the “continuation value” component of  $V_W$  (the HJB part of the variational inequality). It remains to show that the signaling option preserves concavity.

For  $k \geq \phi$ , we have  $V_W(k) = \max(V_W^{\text{cont}}(k), V_H(k - \phi))$ , where  $V_W^{\text{cont}}$  is the continuation value (the solution to the unconstrained HJB). By Step 1,  $V_W^{\text{cont}}$  is strictly concave. By Step 1 applied to regime  $H$ ,  $V_H$  is strictly concave, and hence  $k \mapsto V_H(k - \phi)$  is strictly concave on  $[\phi, \infty)$ . The pointwise maximum of two concave functions is concave (though not necessarily strictly so). Strict concavity of  $V_W$  follows because, at each  $k$ , exactly one of the two functions determines  $V_W$  (by the complementary slackness structure of the variational inequality (24)), and both are strictly concave on their respective active regions. At the boundary  $k^*$ , smooth pasting (25) ensures that  $V_W$  is  $C^1$ , so  $V_W$  is strictly concave on  $(0, \infty)$ . ■

## 15.2. Proof of Proposition 24

PROOF: *Part (i):*  $V_H(k) > V_W(k) > V_L(k)$  for all  $k > 0$ .

We establish the two inequalities separately.

*Step 1:  $V_H(k) > V_L(k)$ .* Fix  $k > 0$  and consider the H-agent mimicking the L-agent’s optimal consumption policy  $\{c_t^L\}$ . Under this strategy, the H-agent’s capital satisfies:

$$dk_t^H = [A_H(k_t^H)^\alpha - c_t^L - \delta k_t^H] dt + \sigma dW_t.$$

Since  $A_H > A_L$  and both agents start at  $k_0 = k$ , the drift is strictly higher at every instant where  $k_t^H > 0$  (which holds almost surely by the reflecting barrier). By the comparison theorem for SDEs with common noise,  $k_t^H \geq k_t^L$  pathwise, and the mimicking strategy is therefore feasible. The H-agent consuming  $\{c_t^L\}$  obtains exactly  $V_L(k)$ . Since mimicking is not optimal—the H-agent can strictly improve by re-optimizing given  $A_H > A_L$ —we conclude  $V_H(k) > V_L(k)$ .

*Step 2:  $V_W(k) > V_L(k)$ .* The W-agent can mimic the L-agent’s consumption policy while ignoring the signaling opportunity entirely. Under this strategy, she produces with  $A_L$  (since

$A_W = A_L$ ) and follows the same capital path as the L-agent. If the opportunity is lost at rate  $\lambda_{HL}$ , she transitions to state L and continues with the L-optimal policy, which she is already following—so the transition has no effect on her payoff. The “ignore the option” strategy therefore yields exactly  $V_L(k)$ . Since  $V_W$  is the supremum over all strategies,  $V_W(k) \geq V_L(k)$ . The inequality is strict for all  $k > 0$  whenever  $k^* < \infty$  (Remark 22, cases (a)–(b)): the signaling option has positive value because there exists a future wealth level at which exercise is optimal, and the positive probability of reaching that level (via drift and diffusion) gives the option strictly positive present value.

*Step 3:*  $V_H(k) > V_W(k)$ . The H-agent is already at productivity  $A_H$  without having to pay any cost. The W-agent produces at  $A_L$  and, to reach  $A_H$ , must pay  $\phi$  at some future date—if she reaches  $k^*$  before the opportunity expires. Formally, consider the H-agent mimicking the W-agent’s optimal strategy (same consumption, same signaling timing if applicable). Since  $A_H > A_L = A_W$ , the H-agent’s capital path dominates the W-agent’s by the same comparison argument as Step 1. Moreover, the H-agent need not pay any signaling cost and faces no risk of losing a pending opportunity. She obtains at least the same consumption stream at strictly lower cost, so  $V_H(k) \geq V_W(k)$ . The inequality is strict because the W-agent operates under  $A_L$  for a positive expected duration before (possibly) reaching  $A_H$ , while the H-agent enjoys  $A_H$  from  $t = 0$ .

*Part (ii):*  $V_W(k) \geq V_H(k - \phi)$  for  $k \geq \phi$ , with equality if and only if  $k \geq k^*$ .

The inequality follows immediately from the definition of  $V_W$ : immediate signaling at  $k \geq \phi$  is an admissible strategy yielding payoff  $V_H(k - \phi)$ , and  $V_W(k)$  is the supremum over all admissible strategies. This is precisely the American constraint in the variational inequality (24).

For the characterization of equality, recall the definition of the signaling surplus  $D(k) = V_W(k) - V_H(k - \phi)$ . In the wait region  $k < k^*$ , the HJB equation binds and  $D(k) > 0$ : the agent strictly prefers to hold the option. In the signal region  $k \geq k^*$ , immediate exercise is optimal:  $V_W(k) = V_H(k - \phi)$  and  $D(k) = 0$ . Therefore  $D(k) = 0$  if and only if  $k \geq k^*$ .

*Part (iii): Full ordering.*

Combining Parts (i) and (ii):

$$V_H(k) > V_W(k) \geq V_H(k - \phi) \quad \text{for } k \geq \phi,$$

with  $V_W(k) = V_H(k - \phi)$  if and only if  $k \geq k^*$ . For  $k < \phi$ , signaling is infeasible and the ordering reduces to  $V_H(k) > V_W(k) > V_L(k)$ . ■

### 15.3. Proof of Proposition 25

PROOF: *Step 1: First-order condition.* The HJB equation for state  $j \in \{L, H\}$  (equations (22) and (23)) requires:

$$\rho V_j = \max_{c>0} \left\{ u(c) + \mu_j(k, c) V_j' + \frac{1}{2} \sigma^2 V_j'' \right\} + \lambda_{\text{out},j} (V_{\text{other}} - V_j),$$

where  $\mu_j(k, c) = f_j(k) - c - \delta k$  is the drift. The first-order condition for the interior maximum over  $c$  is:

$$u'(c_j) = V_j'(k). \tag{41}$$

Under CRRA utility,  $u'(c) = c^{-\gamma}$ , so:

$$c_j(k) = (V'_j(k))^{-1/\gamma}. \quad (42)$$

*Step 2: Differentiate the HJB with respect to  $k$ .* Differentiating the HJB equation (after substituting the optimal  $c_j$ ) with respect to  $k$  yields the *envelope condition*:

$$\rho V'_j = [f'_j(k) - \delta] V'_j + \mu_j V''_j + \frac{1}{2} \sigma^2 V'''_j + \lambda_{\text{out},j} (V'_{\text{other}} - V'_j). \quad (43)$$

This uses the fact that the optimal  $c_j$  satisfies the FOC (41), so the direct effect of  $k$  on  $c_j$  cancels by the envelope theorem (the derivative of the maximand with respect to  $c$  is zero at the optimum).

*Step 3: Apply Itô's lemma to  $V'_j(k_t)$ .* Along the optimal path, the co-state variable  $p_t = V'_j(k_t)$  evolves according to Itô's lemma:

$$dp_t = [\mu_j V''_j + \frac{1}{2} \sigma^2 V'''_j] dt + \sigma V''_j dW_t + (\text{jump terms from regime switching}). \quad (44)$$

Taking expectations and using (43), the expected drift of  $p_t$  is:

$$\mathbb{E}[dp_t]/dt = \rho V'_j - [f'_j(k) - \delta] V'_j - \lambda_{\text{out},j} (V'_{\text{other}} - V'_j). \quad (45)$$

*Step 4: Translate to consumption dynamics.* From the FOC (41),  $p_t = u'(c_j) = c_j^{-\gamma}$ . Differentiating with respect to time:

$$\frac{dp_t}{p_t} = -\gamma \frac{dc_j}{c_j} + \frac{1}{2} \gamma(\gamma + 1) \left( \frac{dc_j}{c_j} \right)^2 + \dots \quad (46)$$

where the second term arises from Itô's correction applied to the nonlinear function  $c^{-\gamma}$ . To obtain the consumption growth rate, we use the chain rule. Since  $c_j = (V'_j)^{-1/\gamma}$ , applying Itô's lemma to  $c_j(k_t)$ :

$$dc_j = c'_j(k) dk_t + \frac{1}{2} c''_j(k) \sigma^2 dt.$$

The expected consumption growth rate is therefore:

$$\frac{\mathbb{E}[dc_j]}{c_j dt} = \frac{c'_j}{c_j} \mu_j + \frac{1}{2} \sigma^2 \frac{c''_j}{c_j}. \quad (47)$$

*Step 5: Combine.* Substituting (45) into the relationship between  $p_t$  and  $c_j$ , and using the FOC (41) to replace  $V'_{\text{other}}$  with  $u'(c_{\text{other}})$ , we obtain after rearranging:

$$\frac{\dot{c}_j}{c_j} = \frac{1}{\gamma} \left[ f'_j(k) - \delta - \rho + \frac{1}{2} \gamma(\gamma + 1) \sigma^2 \frac{c''_j}{c_j} - \lambda_{\text{out},j} \left( 1 - \frac{u'(c_{\text{other}})}{u'(c_j)} \right) \right], \quad (48)$$

where we identify  $\dot{c}_j/c_j$  with the expected consumption growth rate (47) evaluated at the deterministic component of the dynamics. ■

## 15.4. Gauss–Seidel Policy Iteration with American Projection

The coupled HJB system is solved by iterating on the three value functions in sequence, using an implicit time step for stability and an American projection step for the variational inequality in state  $W$ .

**Algorithm 1** Coupled HJB solver with American projection

- 1: **Initialize:** Set  $V_L^0, V_W^0, V_H^0$  (e.g.,  $V_j^0(k_i) = u(f_j(k_i) - \delta k_i)/\rho$ ).
- 2: **for**  $n = 1, 2, \dots$  until convergence **do**
- 3: **Step 1 (L-update):** Compute upwind coefficients  $\{x_i^L, y_i^L, z_i^L\}$  from  $V_L^{n-1}$ . Solve the implicit system:

$$\left(\frac{1}{\Delta t} + \rho - z_i^L + \lambda_{LH}\right) V_{L,i}^n - x_i^L V_{L,i+1}^n - y_i^L V_{L,i-1}^n = \frac{V_{L,i}^{n-1}}{\Delta t} + u(c_{L,i}^{n-1}) + \lambda_{LH} V_{W,i}^{n-1}.$$

This is a tridiagonal system  $A_L \mathbf{V}_L^n = \mathbf{b}_L$ , solved in  $O(N)$  operations.

- 4: **Step 2 (W-update):** Compute upwind coefficients from  $V_W^{n-1}$ . Solve:

$$\left(\frac{1}{\Delta t} + \rho - z_i^W + \lambda_{HL}\right) V_{W,i}^n - x_i^W V_{W,i+1}^n - y_i^W V_{W,i-1}^n = \frac{V_{W,i}^{n-1}}{\Delta t} + u(c_{W,i}^{n-1}) + \lambda_{HL} V_{L,i}^n,$$

where  $V_{L,i}^n$  uses the *just-updated* L-values from Step 1 (Gauss-Seidel ordering).

- 5: **Step 3 (American projection):** For each grid point  $k_i \geq \phi$ , compute the signaling payoff  $v_{\text{sig},i} = V_H^{n-1}(k_i - \phi)$  (interpolating if  $k_i - \phi$  falls between grid points). If  $v_{\text{sig},i} > V_{W,i}^n$ :

$$V_{W,i}^n \leftarrow v_{\text{sig},i},$$

$$\text{signal\_region}(i) \leftarrow \text{true}.$$

Otherwise,  $\text{signal\_region}(i) \leftarrow \text{false}$ .

- 6: **Step 4 (W-policy recomputation):** Recompute the consumption policy  $c_{W,i}^n$ , drift  $\mu_{W,i}^n$ , and upwind coefficients from the *projected*  $V_W^n$ . In the signal region, set  $c_{W,i}^n = c_H^{n-1}(k_i - \phi)$  and  $\mu_{W,i}^n = \mu_H^{n-1}(k_i - \phi)$  (the W-agent who signals behaves as an H-agent at post-signaling wealth).
- 7: **Step 5 (H-update):** Compute upwind coefficients from  $V_H^{n-1}$ . Solve:

$$\left(\frac{1}{\Delta t} + \rho - z_i^H + \lambda_{HL}\right) V_{H,i}^n - x_i^H V_{H,i+1}^n - y_i^H V_{H,i-1}^n = \frac{V_{H,i}^{n-1}}{\Delta t} + u(c_{H,i}^{n-1}) + \lambda_{HL} V_{L,i}^n.$$

- 8: **Step 6 (Convergence check):**  $\varepsilon^n = \max_{j \in \{L, W, H\}} \|V_j^n - V_j^{n-1}\|_\infty$ . Stop if  $\varepsilon^n < \text{tol}$  (typically  $\text{tol} = 10^{-8}$ ).

9: **end for**

- 10: **Output:** Value functions  $\{V_L, V_W, V_H\}$ , consumption policies  $\{c_L, c_W, c_H\}$ , signal region, Skiba threshold  $k^* = k_{\min\{i: \text{signal\_region}(i) = \text{true}\}}$ .

REMARK 37—Gauss-Seidel ordering: The ordering  $L \rightarrow W \rightarrow H$  is chosen to follow the direction of regime transitions: L feeds into W (via  $\lambda_{LH}$ ), W feeds into H (via signaling), and H feeds back into L (via  $\lambda_{HL}$ ). At each step, the most recently updated value function is used

for the neighboring state, which accelerates convergence relative to a Jacobi scheme (where all states use the previous iterate).

REMARK 38—Signal region detection: After the American projection,  $V_W(k_i) \geq V_H(k_i - \phi)$  holds by construction at every grid point. The signaling surplus  $D(k_i) = V_W(k_i) - V_H(k_i - \phi)$  is therefore non-negative everywhere, and using  $D \leq 0$  as the signaling criterion would incorrectly yield “never signal.” The correct indicator is the boolean array `signal_region`, which records where the *unconstrained* solution from Step 2 was overwritten by the projection in Step 3.

REMARK 39—Post-projection policy recomputation: Step 4 is essential for the consistency of the KFE. After the American projection modifies  $V_W$  in the signal region, the consumption policy, drift, and generator coefficients for the W-state must be recomputed from the projected value function. Failing to do so would feed pre-projection policies into the KFE, creating a mismatch between the individual optimization (HJB) and the distributional accounting (KFE). In the signal region, the W-agent’s behavior is identical to an H-agent at wealth  $k - \phi$ : she has already decided to signal, so her consumption and drift are those of state H evaluated at post-signaling capital.

REMARK 40—Implicit time step and convergence speed: The implicit scheme is unconditionally stable: arbitrarily large  $\Delta t$  can be used without numerical instability. In practice, we start with a moderate  $\Delta t$  (e.g.,  $\Delta t = 10$ ) and increase it geometrically as the iteration converges, following [Achdou et al. \(2022\)](#). Under the baseline calibration, the algorithm converges in 8 iterations under this calibration.

### 15.5. Kolmogorov Forward Equation

The stationary wealth distribution is the solution to the Kolmogorov Forward Equation (KFE)—the adjoint of the HJB operator—subject to the non-local transfer induced by signaling. This section derives the discretized KFE system, describes the signaling transfer mechanism, and characterizes the properties of the resulting ergodic distribution.

#### 15.5.1. The Adjoint Operator

DEFINITION 41—Generator and adjoint: The infinitesimal generator of the wealth process in state  $j$  is:

$$\mathcal{L}_j f(k) = \mu_j(k) f'(k) + \frac{1}{2} \sigma^2 f''(k),$$

where  $\mu_j(k) = f_j(k) - c_j(k) - \delta k$  is the optimal drift determined by the HJB system. Its  $L^2$ -adjoint (Fokker–Planck operator) is:

$$\mathcal{L}_j^* g(k) = -\frac{\partial}{\partial k} [\mu_j(k) g(k)] + \frac{1}{2} \sigma^2 \frac{\partial^2 g}{\partial k^2}. \quad (49)$$

The first term represents advection (probability mass is transported by the drift), and the second represents diffusion (probability mass spreads due to Brownian noise).

PROPOSITION 42—Discrete adjoint = transpose: *Let  $L_j$  be the  $N \times N$  HJB generator matrix with entries:*

$$(L_j)_{i,i-1} = y_i, \quad (L_j)_{i,i} = z_i = -(x_i + y_i), \quad (L_j)_{i,i+1} = x_i,$$

where  $x_i, y_i, z_i$  are the upwind coefficients (37)–(39). Then the KFE generator is  $L_j^T$ :

$$(L_j^T)_{i,i-1} = x_{i-1}, \quad (L_j^T)_{i,i} = z_i, \quad (L_j^T)_{i,i+1} = y_{i+1}. \quad (50)$$

The sub- and super-diagonals are swapped relative to the HJB generator: the KFE propagates probability mass in the direction of the drift, while the HJB propagates value against the drift.

PROOF: By definition,  $(L_j^T)_{i,m} = (L_j)_{m,i}$ . The HJB generator has  $(L_j)_{i-1,i} = x_{i-1}$  (the upper-diagonal entry of row  $i-1$ ), so  $(L_j^T)_{i,i-1} = (L_j)_{i-1,i} = x_{i-1}$ . Similarly,  $(L_j^T)_{i,i+1} = (L_j)_{i+1,i} = y_{i+1}$ . ■

REMARK 43—A common numerical error: Using  $L_j$  instead of  $L_j^T$  in the KFE reverses the direction of probability flow: mass is transported *against* the drift rather than with it, causing the density to accumulate at the boundary  $k_{\max}$  instead of concentrating near the interior attractor  $k_j^{ss}$ . This is one of the most frequent implementation errors in HACT models.

### 15.5.2. Boundary Conditions for the KFE

PROPOSITION 44—KFE boundary conditions:

- (i) **Reflecting at  $k=0$ :** The reflecting barrier (Assumption 1(v)) implies zero probability flux at the lower boundary:  $J_j(0) = \mu_j(0)g_j(0) - \frac{1}{2}\sigma^2g_j'(0) = 0$ . In the discretized system, this is enforced by setting  $y_1 = 0$  in the KFE generator (no mass flows below  $k_1$ ).
- (ii) **Vanishing density at  $k = k_{\max}$ :** The zero-drift condition at the upper boundary (Proposition 29) implies that the attractor is interior to the domain. For  $k_{\max}$  sufficiently large, the stationary density is negligible near  $k_{\max}$ :  $g_j(k_{\max}) \approx 0$ . Numerically, this is implemented by setting  $x_N = 0$  in the KFE generator.

### 15.5.3. Non-Local Signaling Transfer

When a W-agent at wealth  $k \geq k^*$  signals, she pays  $\phi$  and arrives in state H at wealth  $k - \phi$ . This is a non-local transfer: probability mass is removed from the W-density at  $k$  and injected into the H-density at  $k - \phi$ , which is generally a different grid point. The implementation requires two components: an outflow mechanism from W and an inflow mechanism to H.

DEFINITION 45—Signaling transfer:

- (i) **Outflow from W.** In the signal region  $\{k_i : \text{signal\_region}(i) = \text{true}\}$  identified by Algorithm 1, the optimal policy is to signal immediately. In the continuous-time model, this means that an agent arriving in W at  $k \geq k^*$  signals instantaneously. Numerically, we approximate instantaneous signaling by a large but finite drain rate  $\bar{\lambda} \gg 1$ :

$$(L_W^T)_{i,i} \leftarrow (L_W^T)_{i,i} - \bar{\lambda} \cdot \mathbf{1}\{i \in \text{signal region}\}. \quad (51)$$

In the limit  $\bar{\lambda} \rightarrow \infty$ , the W-density vanishes in the signal region:  $g_W(k) \rightarrow 0$  for  $k \geq k^*$ . In practice,  $\bar{\lambda} = 10^3$  is sufficient to make  $g_W$  negligible in the signal region without causing numerical instability.

- (ii) **Inflow to H.** Mass drained from W at grid point  $k_i$  arrives in H at  $k_i - \phi$ . Since  $k_i - \phi$  generally falls between two grid points  $k_l$  and  $k_{l+1}$  (where  $k_l \leq k_i - \phi < k_{l+1}$ ), we distribute the inflow using linear interpolation with weight:

$$\omega_i = \frac{(k_i - \phi) - k_l}{\Delta k}, \quad 1 - \omega_i = \frac{k_{l+1} - (k_i - \phi)}{\Delta k}. \quad (52)$$

The transfer matrix  $S$  (dimension  $N \times N$ ) has entries:

$$S_{l,i} = \bar{\lambda}(1 - \omega_i), \quad S_{l+1,i} = \bar{\lambda}\omega_i, \quad (53)$$

for each  $i$  in the signal region, and  $S_{m,i} = 0$  otherwise. The matrix  $S$  appears in the H-block of the KFE as the coupling between the W- and H-densities.

**REMARK 46—Mass conservation:** The transfer preserves total mass: for each signal-region grid point  $i$ , the outflow from W is  $\bar{\lambda}g_{W,i}$  and the total inflow to H is  $S_{l,i}g_{W,i} + S_{l+1,i}g_{W,i} = \bar{\lambda}(1 - \omega_i + \omega_i)g_{W,i} = \bar{\lambda}g_{W,i}$ . No probability mass is created or destroyed by the transfer.

#### 15.5.4. Full Coupled KFE System

**DEFINITION 47—Full KFE matrix:** The stationary distribution  $\mathbf{g} = (\mathbf{g}_L, \mathbf{g}_W, \mathbf{g}_H)^T$  solves the  $3N \times 3N$  linear system  $M\mathbf{g} = \mathbf{0}$ :

$$\underbrace{\begin{pmatrix} L_L^T - \lambda_{LH}I + \lambda_{HL}I_{\text{no-sig}} & \lambda_{HL}I_{\text{no-sig}} & \lambda_{HL}I \\ \lambda_{LH}I & L_W^T - \lambda_{HL}I_{\text{no-sig}} - \bar{\lambda}\text{diag}(\mathbf{1}_{\text{sig}}) & 0 \\ 0 & S & L_H^T - \lambda_{HL}I \end{pmatrix}}_M \begin{pmatrix} \mathbf{g}_L \\ \mathbf{g}_W \\ \mathbf{g}_H \end{pmatrix} = \mathbf{0}, \quad (54)$$

where:

- $L_j^T$  is the transposed HJB generator for state  $j$  (Proposition 42);
- $I_{\text{no-sig}} = \text{diag}(\mathbf{1} - \mathbf{1}_{\text{sig}})$  restricts the  $W \rightarrow L$  flow to the wait region (agents in the signal region exit to H, not to L);
- $\bar{\lambda}\text{diag}(\mathbf{1}_{\text{sig}})$  drains mass from W in the signal region;
- $S$  is the transfer matrix (53) that injects the drained mass into H at post-signaling wealth;
- $\lambda_{HL}I$  in the (1, 3) block captures the obsolescence flow  $H \rightarrow L$ .

**REMARK 48—Flow accounting:** The matrix  $M$  encodes four probability flows:

- L  $\rightarrow$  W** (opportunity arrival): L-agents exit at rate  $\lambda_{LH}$  (block (1, 1), negative term) and enter W (block (2, 1), positive term).
- W  $\rightarrow$  L** (opportunity lost): W-agents in the *wait* region exit at rate  $\lambda_{HL}$  (block (2, 2)) and return to L (block (1, 2)). This flow applies only to agents below  $k^*$  who have not yet signaled.
- W  $\rightarrow$  H** (signaling): W-agents in the *signal* region are drained at rate  $\bar{\lambda}$  (block (2, 2)) and injected into H at wealth  $k - \phi$  via  $S$  (block (3, 2)).
- H  $\rightarrow$  L** (obsolescence): H-agents exit at rate  $\lambda_{HL}$  (block (3, 3)) and return to L (block (1, 3)).

Each flow conserves mass: what exits one state enters another. The total mass  $\sum_j \mathbf{1}^T \mathbf{g}_j$  is preserved, as can be verified by summing the columns of  $M$ .

The normalization condition

$$\Delta k \sum_{i=1}^N [g_{L,i} + g_{W,i} + g_{H,i}] = 1 \quad (55)$$

is imposed by replacing one row of  $M$  (typically the last) with  $\Delta k \cdot \mathbf{1}^T$ , yielding a non-singular system with a unique solution.

### 15.5.5. Properties of the Stationary Distribution

PROPOSITION 49—Stationary distribution: *Under the conditions of Proposition 32, the system (54)–(55) admits a unique non-negative solution  $\mathbf{g} = (\mathbf{g}_L, \mathbf{g}_W, \mathbf{g}_H)$  with the following properties:*

- (i) *Bimodal total density. The aggregate density  $g(k) = g_L(k) + g_W(k) + g_H(k)$  has two local maxima: one near  $k_L^{ss,c}$  and one near  $k_H^{ss,c}$ .*
- (ii) *State-specific concentration.  $g_L$  is concentrated near  $k_L^{ss,c}$  with a right tail extending above  $k_L^{ss,c}$  (generated by  $H \rightarrow L$  transitions of agents with  $k > k_L^{ss,c}$  who then decumulate).  $g_H$  is concentrated near  $k_H^{ss,c}$  with a left tail extending below  $k_H^{ss,c}$  (generated by  $W \rightarrow H$  transitions of agents entering at  $k^* - \phi < k_H^{ss,c}$  who then accumulate).*
- (iii) *Negligible W-density in the signal region. For  $k \geq k^*$ ,  $g_W(k) \approx 0$ : agents who reach the Skiba threshold signal immediately (or, in the numerical implementation, at rate  $\bar{\lambda}$ ), so no mass accumulates above  $k^*$  in state W.*
- (iv) *Positive W-density in the wait region. For  $k \in (0, k^*)$ ,  $g_W(k) > 0$ : these are the “Frustrated Aspirants” who have received the signaling opportunity but are accumulating toward  $k^*$ .*
- (v) *Ergodic shares. The long-run population fractions  $\pi_j = \int_0^{k^{\max}} g_j(k) dk$  depend on all model parameters. In the limiting case where signaling is instantaneous ( $k^* = \phi$ , so that  $\pi_W \approx 0$ ), the shares reduce to:*

$$\pi_L \approx \frac{\lambda_{HL}}{\lambda_{LH} + \lambda_{HL}}, \quad \pi_H \approx \frac{\lambda_{LH}}{\lambda_{LH} + \lambda_{HL}}.$$

*When  $k^* > \phi$ , the delay in signaling increases  $\pi_L + \pi_W$  at the expense of  $\pi_H$ : some agents who receive the opportunity never signal (they lose it before reaching  $k^*$ ), reducing the effective flow into state H.*

PROOF SKETCH: The matrix  $M$  with the normalization row replaced is a non-singular M-matrix (by the monotonicity of the upwind scheme and the positivity of the switching and drain rates), so the system has a unique solution. Non-negativity of  $\mathbf{g}$  follows from the M-matrix property (the inverse of an M-matrix has non-negative entries). Properties (i)–(iv) follow from the attractor structure: near each  $k_j^{ss,c}$ , the drift  $\mu_j$  is approximately linear with negative slope ( $\mu'_j(k_j^{ss,c}) < 0$ ), which concentrates mass near the attractor. The tails in (ii) are generated by the regime-switching terms, which inject mass at points away from the attractors. Property (v) follows from balancing the steady-state flows: in the long run, the inflow to each state must equal the outflow. ■

REMARK 50—Metastability: Although the stationary distribution is unique (the economy is ergodic), convergence to stationarity can be extremely slow. The mixing time—the time required for an agent’s distribution to approach the ergodic distribution regardless of initial conditions—scales exponentially with the squared distance between attractors in the small-noise limit (Kramers’ escape rate). Under our baseline calibration, the diffusion-driven mixing time exceeds 150 years. The regime-switching channel ( $L \rightarrow W \rightarrow H$  and  $H \rightarrow L$ ) provides a faster route between basins, but even this channel operates on a time scale of  $1/(\lambda_{LH} + T_{acc}) \approx 10$ –20 years. The economy therefore exhibits *metastability*: it is theoretically ergodic but practically polarized on policy-relevant time horizons.

15.6. Discussion of Key Parameters

*Preferences* ( $\gamma, \rho$ ). The coefficient of relative risk aversion  $\gamma = 2$  is a standard benchmark in the macroeconomics and finance literature, lying in the middle of the range  $\gamma \in [1, 5]$  considered empirically plausible (Lucas, 1987, Attanasio, 1999, Chetty, 2006). The discount rate  $\rho = 0.05$  is conventional for annual calibrations in the HACT literature (Achdou et al., 2022, Kaplan et al., 2018) and implies moderate impatience.

*Technology* ( $\alpha, \delta$ ). The curvature parameter  $\alpha = 0.33$  governs the degree of diminishing returns at the individual level. We adopt this value for consistency with the macroeconomic literature, where  $\alpha \approx 1/3$  is the standard calibration of the capital elasticity in Cobb-Douglas specifications. In our framework,  $\alpha$  plays a central role: it determines the location of the attractors through the zero-drift condition  $f'_j(k_j^{ss,c}) - \delta = \rho$ , and it controls the curvature of the value function near the steady state, which in turn governs the MPC. We explore the sensitivity to  $\alpha$  in the comparative statics of Section 13.2.

The depreciation rate  $\delta = 0.02$  is low relative to the standard calibration for physical equipment ( $\delta \approx 0.05\text{--}0.10$ ). We choose this value for two reasons. First, in the model, capital  $k$  is best interpreted as productive capacity broadly defined—the bundle of physical assets, skills, and market access that determines an agent’s income under technology  $A_j$ . The non-physical components of this bundle depreciate more slowly than machinery. Second, and more importantly, the ratio  $\rho/(\rho + \delta)$  governs the attractor locations: a low  $\delta$  places the attractors at capital levels where the poverty trap dynamics—the wait zone, the signaling cost relative to  $k_L^{ss,c}$ , and the MPC/APC diagnostics—are clearly visible in the numerical output. Section 13.2 verifies that the qualitative results are robust to higher values of  $\delta$ .

*TFP gap* ( $A_H/A_L$ ). We set  $A_H/A_L = 1.25$ , implying a 25% productivity advantage for agents who have successfully signaled. This is a conservative choice. The empirical literature on the returns to credentials and technology adoption suggests substantially larger gaps: the college wage premium in the United States is approximately 60–80% (Goldin and Katz, 2008), and productivity differentials between formal and informal sector workers in developing economies range from 30% to over 100% (La Porta and Shleifer, 2014). We deliberately choose a moderate gap for two reasons. First, not all of the observed wage premium reflects a TFP difference—part is a return to unobserved ability, sorting, or complementarity with other inputs. Second, a smaller gap makes the bimodality result more demanding: the model must generate Twin Peaks despite relatively close attractors, which strengthens the case that the signaling friction—not an implausibly large technology difference—is driving the polarization.

Under this calibration, the deterministic steady states are:

$$k_L^{ss}(0) = \left( \frac{\alpha A_L}{\rho + \delta} \right)^{1/(1-\alpha)} \approx 10.12, \quad k_H^{ss}(0) = \left( \frac{\alpha A_H}{\rho + \delta} \right)^{1/(1-\alpha)} \approx 14.12, \quad (56)$$

yielding a deterministic separation of approximately 4.0 capital units. In the full stochastic coupled model, precautionary savings, option-value effects, and regime coupling shift both attractors (Propositions 6, 8, and 10). *Diffusion* ( $\sigma$ ). The additive noise parameter  $\sigma = 0.30$  gov-

erns the dispersion of wealth around each attractor. With additive noise, the standard deviation of wealth near  $k_j^{ss}$  is approximately  $\sigma_j^{ss} \approx \sigma / \sqrt{2|\mu'_j(k_j^{ss})|}$ , which under our calibration yields local standard deviations of order 1–2 capital units. The parameter is chosen to produce realistic wealth dispersion within each basin while maintaining sufficient separation for bimodality (condition (C2) of Proposition 32). The additive specification is discussed in Remark 2.

*Switching rates* ( $\lambda_{LH}$ ,  $\lambda_{HL}$ ). The opportunity arrival rate  $\lambda_{LH} = 0.005$  and the obsolescence rate  $\lambda_{HL} = 0.002$  are deliberately small, producing slow turnover between productivity regimes. Taken literally, they imply a mean waiting time of  $1/\lambda_{LH} = 200$  years before a signaling opportunity arrives and a mean H-regime duration of  $1/\lambda_{HL} = 500$  years. These figures should not be read as individual lifespans but as reflecting the Schumpeterian nature of the underlying shocks.

In Schumpeter’s framework, economic progress is punctuated by long waves of creation and destruction: the transitions from steam to electricity, from electromechanical to digital, or from analog to AI-driven production each unfold over decades and reshape the entire occupational structure. In our model,  $\lambda_{LH}$  captures the rate at which such paradigm shifts *create* new pathways for upward mobility—the opening of a training program, the emergence of a credential with market value, or a regulatory reform that makes a previously inaccessible sector contestable. The rate  $\lambda_{HL}$  captures the symmetric process of *destruction*: the obsolescence of a once-valuable specialization, the automation of a routine task, or the commoditization of a previously scarce skill. Both processes operate on generational timescales, consistent with the empirical observation that poverty traps persist across generations (Azariadis and Stachurski, 2005) and that major technological transitions take 30–60 years to fully diffuse through the economy (Comin and Hobijn, 2010).

Two clarifications are in order. First, the individual interpretation overstates the persistence because the model is ergodic: what matters for the stationary distribution is not the individual waiting time but the *flow rate* between basins. In steady state,  $\lambda_{LH} \cdot \pi_L$  agents transition per unit time from L to W, and  $\lambda_{HL} \cdot (\pi_W + \pi_H)$  from  $\{W, H\}$  to L. Under the baseline calibration, these flows produce ergodic shares of  $\pi_L = 25.2\%$ ,  $\pi_W = 11.8\%$ , and  $\pi_H = 63.0\%$ —a cross-sectional composition that is empirically plausible even though the underlying individual rates are slow.

Second, the small rates are required by the moderate coupling condition (C3) of Section 7: with  $\lambda_{LH}, \lambda_{HL} \ll 1$ , agents remain in each basin long enough for the local attractor to concentrate mass into a distinguishable mode. Raising the rates accelerates turnover and eventually merges the two peaks into a single mode, destroying the bimodal structure. The comparative statics of Section 13.2 quantify this threshold.

*Signaling cost* ( $\phi$ ). The cost  $\phi = 9.0$  is calibrated to produce an interior Skiba threshold. Under the baseline parameters,  $\phi < k_L^{ss,c}$ : the signaling cost is below but close to the L-attractor, so an L-agent who receives an opportunity can afford to signal but may find it suboptimal to do so immediately (because post-signaling wealth  $k - \phi$  is too low to sustain the transition profitably). She must accumulate further from  $k_L^{ss,c}$  to the Skiba threshold  $k^*$ . This generates a meaningful wait zone  $[\phi, k^*)$  populated by Frustrated Aspirants.

In economic terms,  $\phi$  represents the total cost of credential acquisition—tuition, forgone income, and the direct utility cost of the signaling process. With  $k_L^{ss}(0) \approx 10.12$  and  $\phi = 9.0$ , the signaling cost is approximately 89% of the L-agent’s deterministic steady-state capital, roughly comparable to the ratio of four-year college costs to median household wealth documented by Goldin and Katz (2008).

### 15.6.1. Summary of the Numerical Experiment

The numerical experiment proceeds as follows:

- (i) *HJB solution* (Algorithm 1): The coupled HJB system is solved on a uniform grid of  $N = 501$  points over  $[0.01, 50]$  using implicit policy iteration with  $\Delta t = 500$ , until the sup-norm error falls below  $10^{-8}$ . The algorithm converges in 8 iterations.

- (ii) *Skiba detection*: The signal region is identified from the American projection step. The Skiba threshold  $k^*$  is the lowest grid point at which the constraint  $V_W(k) \geq V_H(k - \phi)$  binds.
- (iii) *KFE solution*: The stationary distribution is obtained by solving the  $3N \times 3N$  linear system (54) with normalization (55). The signaling drain rate is  $\bar{\lambda} = 10^3$ .
- (iv) *Distributional diagnostics*: We compute the ergodic shares  $(\pi_L, \pi_W, \pi_H)$ , the mean wealth  $\mathbb{E}[k]$ , and the Gini coefficient from the stationary distribution.